UNIVERSITY
OF MICHIGAN
SEP 2 6 1950
ENGINEERING
LIBRARY

THE AERONAUTICAL QUARTERLY

Volume II AUGUST 1950 Part II

CONTENTS

Critical Mach Numbers for Swept-Back Wings — *S. Neumark*

General Performance Reduction Equations for Reciprocating-Engined Aircraft with Constant-Speed Propellers — *W. J. D. Annand*

The Axially-Symmetrical Supersonic Flow Near the Centre of an Expansion — *N. H. Johannesen and R. E. Meyer*

Note on the Dependence of Flap Hinge Moment Derivatives on Hinge Position — *W. J. Duncan*

On the Chordwise Lift Distribution at the Centre of Swept Wings — *D. Kuchemann and J. Weber*

Amendments to "A Note on the Bending Moment Induced in the Booms of a Spar at the point of Application of a Concentrated Load" (Volume I, Part IV) — *H. F. Winny*

LONDON
ROYAL AERONAUTICAL SOCIETY
4 HAMILTON PLACE W1

10/-

THE AERONAUTICAL QUARTERLY

Editorial Board

W. G. A. PERRING, C.B., F.R.Ae.S. (*Chairman*)

Dr. H. ROXBEE COX, D.I.C., F.R.Ae.S., F.I.Ae.S.

Professor S. GOLDSTEIN, F.R.S., F.R.Ae.S.

Sir GEOFFREY TAYLOR, F.R.S.

G. H. DOWTY, F.R.Ae.S. (Chairman of the JOURNAL Committee of the Royal Aeronautical Society)

J. SMITH, C.B.E., F.R.Ae.S., A.M.I.Mech.E. (Chairman of the Technical Board and Executive Committee of the Society of British Aircraft Constructors)

Joint Editors

Captain J. Laurence Pritchard, Hon.F.R.Ae.S., Hon.F.I.Ae.S.
Joan Bradbrooke, A.R.Ae.S.

Editorial Referees

Aerodynamics

(a) *General*

Prof. L. BAIRSTOW
Dr. G. P. DOUGLAS
Prof. A. A. HALL
Sir B. MELVILL JONES
Mr. D. KEITH-LUCAS
Dr. N. A. V. PIERCY
Mr. W. G. A. PERRING
Mr. R. F. RELF
Mr. B. J. RICHARDS

(b) *Field Motion*

Mr. A. FAGE
Prof. S. GOLDSTEIN
Prof. L. HOWARTH
Mr. W. P. JONES
Dr. J. W. MACCOLL
Dr. J. H. PERETTIE
Mr. L. F. G. SIMMONDS
Mr. H. B. SQUIRE
Sir GEOFFREY TAYLOR
Prof. G. TEMPLE
Mr. A. D. YOUNG

(c) *Stability and Control*

Mr. L. W. BRYANT
Mr. S. B. GATES
Mr. G. T. R. HILL
Mr. H. B. IRVING
Mr. G. H. LEE
Mr. M. B. MORGAN

Helicopters and Propellers

Dr. J. A. J. BENNETT
Mr. L. G. FAIRHURST
Mr. R. HAFNER
Capt. R. N. LIPTROT

Instrumental and Electrical Equipment

Dr. G. E. BAIESTO
Mr. G. W. H. GARDINER
Mr. C. S. HUDSON
Mr. A. N. IRBY
Mr. C. N. JAQUES
Mr. F. W. MERRIDETH

Aircraft Design

Mr. R. BOOKMAN
Mr. R. M. CLARKSON
Mr. A. E. CLIFTON
Mr. W. S. FARREN
Mr. H. H. GARDNER
Mr. H. KNOWLES
Mr. W. R. W. PETTER
Mr. F. H. POLLICUTT
Mr. A. R. RUSSELL
Mr. R. S. STAFFORD

Radio and Radar

Mr. J. F. ATHERTON
Mr. B. G. GATES
Mr. R. L. SMITH ROSE
Dr. A. M. UTTLEY
Sir ROBERT WATSON WATT

Aviation Medicine

Dr. A. BUCHANAN BARBOUR

Meteorology

Prof. D. BRUNT
Mr. J. K. HAMDY
Prof. P. A. SHEPPARD

Aircraft Propulsion

Mr. H. CONSTANT
Sir A. H. ROY FEILDEN
Dr. S. HOOKER
Mr. P. LLOYD
Dr. A. W. MORLEY
Dr. E. S. MOULT
Mr. N. S. MUIR
Mr. F. NIXON
Mr. F. M. OWNER
Dr. D. PYE
Mr. H. SAMSONOW
Prof. O. A. SAUNDERS

Air Transport

Mr. P. G. MASEFIELD
Mr. N. E. ROWE
Mr. W. TYE

Aircraft Accessories

Mr. W. C. CLOTHIER
Mr. H. O. CONWAY
Mr. G. H. DOWTY
Mr. R. GRAHAM

Vibration and Flutter

Prof. A. R. COLLAR
Prof. W. J. DUNCAN
Mr. R. A. FRAZER
Mr. J. HANSON
Mr. A. ROBINSON

Performance

Mr. H. DAVIES
Mr. D. R. NEWMAN
Mr. A. H. YATES

Structures

Mr. A. C. BROWN
Mr. H. L. COX
Mr. D. J. FARRAR
Dr. H. ROXBEE COX
Mr. W. S. HEMP
Mr. E. B. HOWARD
Mr. E. D. KEL-
Mr. F. A. KERRY
Dr. D. M. A. LEGGETT
Prof. R. L. LICKLEY
Prof. A. J. SUTTON PIPPARD
Prof. A. G. PUGSLEY
Dr. S. C. REDSHAW
Mr. R. H. SANDIFER
Sir RICHARD SOUTHWELL

Fuels and Oils

Mr. E. L. BASS
Mr. J. W. DRINKWATER
Prof. F. H. GARNER
Prof. W. E. GARNER
Dr. K. B. W. RIDDER
Dr. C. G. WILLIAMS

Materials

Prof. L. AITCHISON
Dr. N. P. ALLEN
Prof. N. F. MOTT
Mr. L. ROTHERHAM
Dr. H. SUTTON
Dr. C. SYKES

Flight Testing

Mr. P. A. HUFTON
Mr. E. T. JONES
Mr. S. SCOTT HALL
Mr. H. L. STEVENS

CRITICAL MACH NUMBERS FOR SWEPT-BACK WINGS*

by

S. NEUMARK, Tech.Sc.D., A.F.R.Ae.S., A.F.I.Ae.S.
(Aerodynamics Department, Royal Aircraft Establishment)

INTRODUCTION AND SUMMARY

The effect of yawing a wing in high-speed flow is to delay the onset of shock waves and to increase the critical Mach number. This is because shock waves can only develop along the isobars (running parallel to the edges of the wing, which is assumed untapered and infinitely long), and therefore only the velocity component normal to the edges is significant. To some extent the same is true for a finite sheared or swept-back wing, though the problem is made more complicated by the various additional factors, such as finite aspect ratio (tip effect), plan form (*e.g.* taper effect) and, what is perhaps the most important, the central kink effect. The experimental technique is extremely cumbersome because of the many shape parameters involved (*see* Figs. 1, 2, 3), and since analytical solutions present fundamental difficulties and pitfalls, designers tend to favour rule of thumb methods. The present paper contains a general review of the theoretical work done at The Royal Aircraft Establishment, which was limited to the case of zero incidence. This limitation is not a severe one, as flight at high speeds often implies low incidence. Incidences which are not negligible involve the solution of another fundamental problem (that of the lift distribution).

The results presented here do not depend on lift theories, and belong entirely to the field of classical hydrodynamics. The method used is that of sources and sinks and is really a linear perturbation theory for thin aerofoils. The early results obtained were confined to the kink effect and referred primarily to infinite aspect ratio. It is felt now that the fundamental mathematical difficulties connected with the kink, tips and taper have been satisfactorily overcome, and the results are shown in the series of curves presented. These give velocity (and hence pressure) distributions, the course of the isobars, and critical Mach numbers as functions of geometric parameters. For a finite swept-back wing the central kink section is

Paper received November 1948.

*Paper presented to Section 2, VIIth International Congress of Applied Mechanics, London, September 1948.

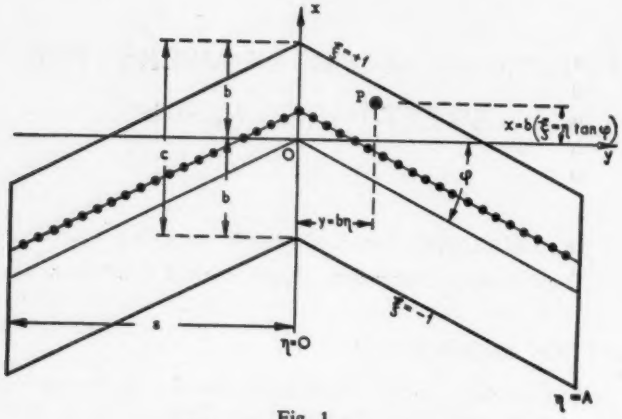

Fig. 1.
Untapered swept-back wing.

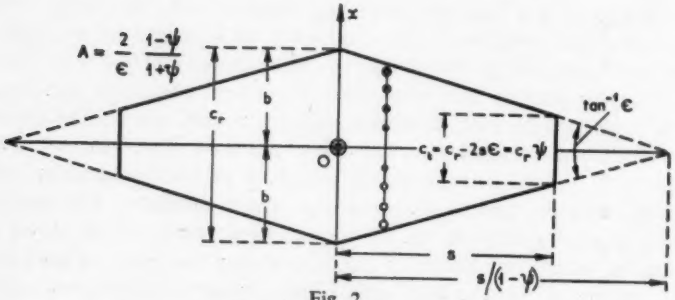

Fig. 2.
Tapered unswept wing.

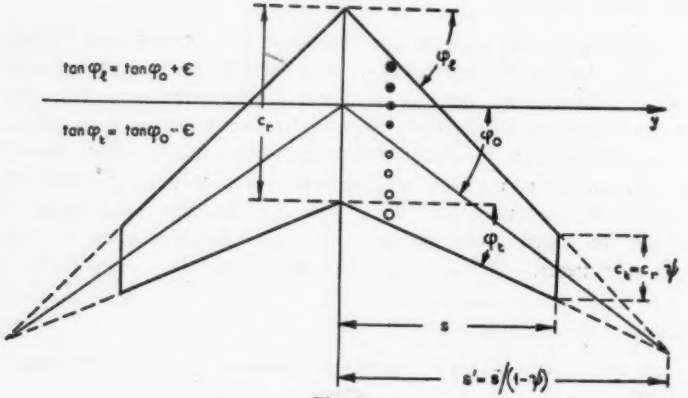

Fig. 3.
Tapered swept-back wing.

normally the first danger zone, and the lower critical Mach number is defined as that corresponding to the flow reaching sonic characteristics locally in this section. With increasing Mach number the sonic region gradually expands spanwise, and the upper critical Mach number is the one above which shock waves may cover almost the entire wing. The tips are often immune up to even higher speeds.

The effect of sweepback is of great practical interest since it seems to make possible flight at very high subsonic or even low supersonic speeds, while retaining essentially subsonic aerodynamic characteristics.

Notation

A	aspect ratio of complete swept-back wing (or double the aspect ratio of a finite sheared wing)
a	speed of sound
a_0	speed of sound in undisturbed flow
b	half-chord of wing section (Fig. 1)
C_D	local drag coefficient in potential flow
c	chord of wing section
c_r	root chord (Figs. 2 and 3)
c_t	tip chord (Figs. 2 and 3)
$F(x)$	function determining wing section
$F'(x)$	first derivative of $F(x)$
$f(x, y)$	function determining wing surface
$f'_x(x, y)$	first partial derivative of $f(x, y)$ with respect to x
G	ratio of the true local supervelocity at any point of the surface of an untapered swept-back wing to the maximum supervelocity on an infinite sheared wing of the same section and angle of sweepback
G'	value of G for the "Göthert wing"
G_{max}	maximum value of G
M	Mach number of undisturbed flow (or flight Mach number)
M_{cr}	critical Mach number
q	local source strength
r_1, r_2	auxiliary symbols, defined in (17)
s	semi-span

t	thickness of wing section
t'	value of t for the "Göthert wing" (Fig. 23)
U	undisturbed velocity of air flow (velocity of flight)
V	resultant velocity on wing surface
V_n	velocity component normal to the leading and trailing edges of an untapered sheared or swept-back wing
v_x, v_y, v_z	velocity components induced by a system of sources and sinks representing a wing
x, y, z	rectangular co-ordinates (x chordwise, positive forwards; y spanwise, positive to starboard; z vertical, positive upwards)
$\bar{x}$	chordwise co-ordinate of source filament
x^*, y^*	co-ordinates of a source element in the x, y-plane
$Y=y/s$	auxiliary variable (*see* (24))
γ	adiabatic constant ($\simeq 1.4$)
$\delta=\lvert v_x/U \rvert_{max}$	maximum supervelocity ratio in incompressible flow
δ'	value of δ for the "Göthert wing" (Fig. 23)
ε	coefficient of convergence of a tapered wing (Figs. 2 and 3)
ν	ratio of the section area to that of a circumscribed rectangle
ξ, η	non-dimensional co-ordinates in the x, y-plane (*see* (17))
ξ_m	value of ξ in the central kink section at the point where the supervelocity attains its maximum
φ	angle of sweepback
φ_0	angle of sweepback of mid-chord line (Fig. 3)
φ_l	angle of sweepback of leading edge (Fig. 3)
φ_t	angle of sweepback of trailing edge (Fig. 3)
φ'	angle of sweepback of the "Göthert wing" (Fig. 23)
$\psi=c_t/c_r$	taper ratio
$\vartheta=t/c$	thickness ratio of wing section

PART I

VELOCITY DISTRIBUTIONS AT ZERO INCIDENCE IN INCOMPRESSIBLE FLOW

The problem of finding the velocity distribution on a swept-back wing being essentially three-dimensional, there is little hope of solving it exactly by potential flow theory. The only suitable approach seems to be the approximate first order method (usually called "linear perturbation theory") in which the wing is replaced by an approximate continuous system of sources and sinks, and the velocities

induced by such a system are calculated. The field of these induced velocities must then be superimposed on that of the undisturbed uniform velocity U. If the induced velocity components are denoted by v_x, v_y, v_z, the resultant velocity V is given by

$$V^2=(-U+v_x)^2+v_y^2+v_z^2. \quad . \quad . \quad . \quad . \quad . \quad (1)$$

All three induced velocity components are small of the first order, and the resultant velocity, to the same order of accuracy, is

$$V \simeq -U+v_x. \quad . \quad . \quad . \quad . \quad . \quad (2)$$

This is the value to use when finding either local pressure or the shape of the isobars, but for determining critical Mach number the component v_y may be as important as v_x.

The linear perturbation theory has been applied successfully by many authors to the two-dimensional case, *i.e.* to a straight wing of infinite aspect ratio. In this case the local source strength q (per unit area) at any point of the chord is proportion to the local slope of the wing section, that is

$$q=-2UF'(x). \quad . \quad . \quad . \quad . \quad . \quad (3)$$

where $z=F(x)$ is the equation of the upper arc of the wing section.

The infinitesimal induced velocity components dv_x and dv_y contributed by one single source filament are shown in Fig. 4. The total induced velocity components are obtained by integration, and it can be proved that for a thin wing, the total v_z, whether calculated at a point P on the surface or at its projection Q on the chord, is, to the required order of accuracy,

$$\lim_{z\to 0} v_z=-UF'(x). \quad . \quad . \quad . \quad . \quad . \quad (4)$$

Hence the boundary conditions are satisfied, to the same order or accuracy. The supervelocity v_x is then determined by integration, and it is again sufficient to calculate it at the point Q using the formula

$$v_x=-\frac{U}{\pi}\int_{-b}^{b}\frac{F'(\bar{x})}{x-\bar{x}}\,d\bar{x}. \quad . \quad . \quad . \quad . \quad . \quad (5)$$

The integral involved is improper, and its principal value should be taken. Thus the supervelocity distribution is determined, in the most general case, directly from the equation of the section.

The example in Fig. 4 refers to the simplest "bi-convex parabolic section," given by

$$z=F(x)=\tfrac{1}{2}t\left(1-\frac{x^2}{b^2}\right). \qquad . \quad . \quad . \quad . \quad (6)$$

The source and sink distribution is linear in this case (Fig. 4), and the supervelocity becomes

$$v_x=-\frac{4}{\pi}U\vartheta\left(1-\tfrac{1}{2}\xi\log_e\frac{1+\xi}{1-\xi}\right), \qquad . \quad . \quad (7)$$

where $\vartheta=t/c$ is the thickness ratio, and $\xi=x/b$ is the non-dimensional chordwise co-ordinate, which is equal to -1 at the trailing edge and $+1$ at the leading edge. The chordwise supervelocity distribution is shown in the lower diagram of Fig. 4.

Similar solutions can be obtained for an arbitrary section shape. Their accuracy is quite good for thin sections, though singularities usually occur at both the leading and trailing edges. The important maximum values of v_x obtained by this method are sufficiently accurate for all practical purposes. In the given case $|v_x|_{max}$ occurs exactly at the mid-point of the chord, and the maximum supervelocity ratio is

$$\delta=\left|\frac{v_x}{U}\right|_{max}=\frac{4}{\pi}\vartheta\simeq 1.27\,\vartheta. \qquad . \quad . \quad . \quad . \quad (8)$$

For an elliptic section it may be noticed that $\delta=\vartheta$, this being almost the minimum supervelocity ratio obtainable, and, from the point of view of critical Mach number, it is important to keep the ratio δ/ϑ as small as possible. It will always exceed unity and will usually be greater than 1.2.

If δ is determined for any section, the maximum total velocity is

$$V_{max}=U(1+\delta), \qquad . \quad . \quad . \quad . \quad . \quad (9)$$

and the condition for critical Mach number is obtained by equating this expression (transformed to allow for compressibility) to the local speed of sound. (For the results *see* Part II).

Since the method of sources and sinks is so effective in the two-dimensional problem, it is logical to try to apply it to three-dimensional cases, especially for swept-back wings. In the general case of a thin wing with arbitrary plan form and arbitrary distribution of (symmetrical) sections, the plan form area S will be defined in terms of x and y, while the upper surface of the wing is represented by the equation

$$z=f(x, y). \qquad . \quad . \quad . \quad . \quad . \quad . \quad (10)$$

(x, y within S).

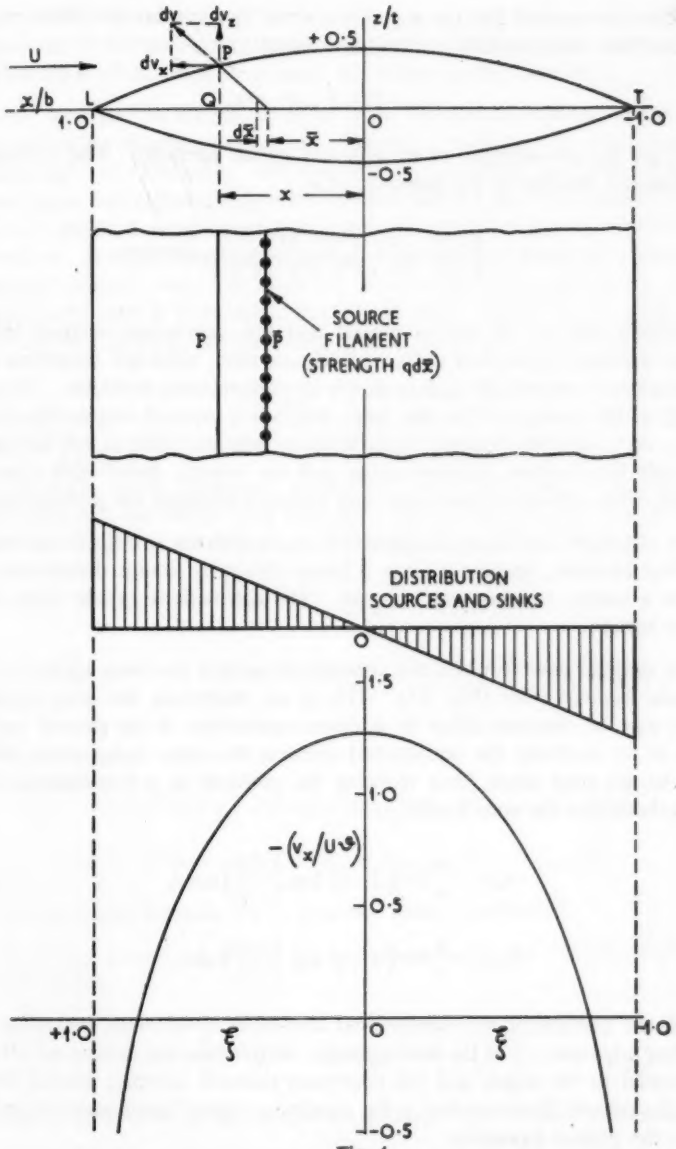

Fig. 4.
Distribution of sources and induced velocity for a straight wing with bi-convex parabolic section.

It may then be assumed that the area S is covered by a continuous system of sources and sinks, their local intensity per unit area being

$$q = -2U \cdot f'_x(x^*, y^*), \quad . \quad . \quad . \quad . \quad . \quad (11)$$

(x^*, y^*, are the co-ordinates of an arbitrary source element). The v_x component of the induced velocity at any point (x, y) is

$$v_x = -\frac{U}{2\pi} \iint_S \frac{(x-x^*) \cdot f'(x^*, y^*)}{\{(x-x^*)^2 + (y-y^*)^2\}^{\frac{3}{2}}} dx^* dy^*, \quad . \quad . \quad . \quad (12)$$

and similarly for v_y. It can be proved that this generalised method still gives solutions accurate to the first order of thickness ratio, although the errors may be somewhat larger numerically than in simple two-dimensional problems. The method fails only at the contour of the plan form, which is a locus of singularities on which either v_x or v_y or both become logarithmically infinite. This is not serious, as it affects only very narrow marginal strips, and the velocity distribution over almost the entire wing surface is represented with sufficient accuracy for practical purposes.

For simplicity the bi-convex parabolic section shown in Fig. 4 has been used in the first instance, because it gives a linear chordwise source distribution and is therefore a perfect "guinea pig" section. The calculations can be made for any arbitrary section.

The simplest case to which the generalised method has been applied is that of an infinite sheared wing (Fig. 21). This is an interesting test case because the solution may be obtained either by a direct application of the general method of sources or by resolving the undisturbed uniform flow into components along and normal to the wing edges, thus reducing the problem to a two-dimensional one. Both methods give the same results, *i.e.*

$$v_x = -\frac{4}{\pi} U\vartheta \left(1 - \tfrac{1}{2}\xi \log_e \frac{1+\xi}{1-\xi}\right) \cos\varphi, \quad . \quad . \quad . \quad (13)$$

$$v_y = -\frac{4}{\pi} U\vartheta \left(1 - \tfrac{1}{2}\xi \log_e \frac{1+\xi}{1-\xi}\right) \sin\varphi. \quad . \quad . \quad . \quad (13a)$$

ξ is still the convenient non-dimensional chordwise co-ordinate, becoming -1 at the trailing edge and $+1$ at the leading edge. In this case the isobars are all straight lines parallel to the edges, and the *maximum relevant velocity*, needed for determining the critical Mach number, is the maximum normal component (at mid-chord point in the present example)

$$(V_n)_{max} = U(\cos\varphi + \delta). \quad . \quad . \quad . \quad (14)$$

Comparison of this relation with equation (9) shows that, because of the presence of the term $\cos\varphi$, $(V_x)_{max}$ can be reduced by increasing the sweepback.

The next step in the theory is to apply the general method to the case of a *swept-back wing of infinite aspect ratio* (*see* Fig. 1 with $s=\infty$), as first suggested by H. Ludwieg[7] of Göttingen. His method was essentially the same as that of the present paper, but unfortunately it led him to a false result. He assumed rightly that for such a wing the danger zone was at the kink, and he confined his calculation to this section. A simple integration brought him back to formula (13), exactly as for an infinite sheared wing, but he failed to notice the full paradoxical meaning of his result, and used it to calculate the critical Mach number in the danger section. According to Ludwieg, the maximum total velocity in the kink section would be

$$|V|_{max}=U(1+\delta\cos\varphi), \quad . \quad . \quad . \quad . \quad . \quad (15)$$

δ being the maximum supervelocity ratio in the two-dimensional case.

Ludwieg's error remained unnoticed until calculations of the velocity distribution over the whole wing area were made at the Royal Aircraft Establishment. The result was the following, regrettably complicated, formula

$$v_x=-\frac{4}{\pi}U\vartheta\cos\varphi\left\{1-\tfrac{1}{2}\xi\log_e\frac{1+\xi+(r_1-\eta)\tan\varphi}{1-\xi-(r_2-\eta)\tan\varphi}+\right.$$
$$\left.+\tfrac{1}{2}\eta\tan\varphi.\log_e\frac{r_1+(1+\xi)\sin\varphi\cos\varphi+\eta\cos 2\varphi}{r_2-(1-\xi)\sin\varphi\cos\varphi+\eta\cos 2\varphi}\right\}, \quad . \quad (16)$$

where

$$\left.\begin{aligned} r_1&=\sqrt{\{(1+\xi)^2\cos^2\varphi-2(1+\xi)\eta\sin\varphi\cos\varphi+\eta^2\}}, \quad \xi=\frac{x+y\tan\varphi}{b}\\ r_2&=\sqrt{\{(1-\xi)^2\cos^2\varphi+2(1-\xi)\eta\sin\varphi\cos\varphi+\eta^2\}}, \quad \eta=y/b \end{aligned}\right\}. \quad (17)$$

The corresponding formula for v_y was still more complicated.

Assuming $\eta\longrightarrow 0$ we obtain the true formula for the velocity distribution at the kink section

$$v_x=-\frac{4}{\pi}U\vartheta\left\{1-\tfrac{1}{2}\xi\log_e\left(\frac{1-\xi}{1+\xi}\,\frac{1-\sin\varphi}{1+\sin\varphi}\right)\right\}\cos\varphi. \quad . \quad . \quad (18)$$

This differs from (13) by the factor $(1+\sin\varphi)/(1-\sin\varphi)$ inside the bracket.

The difference is due to Ludwieg's assumption that $\eta=0$ before the final integration, while the reverse procedure is adopted here. A mathematical singularity,

connected with the geometrical discontinuity in plan form, implies that "the limit of an integral" is not equal to "the integral of a limit." Because of this Ludwieg missed what we now call "kink effect."

The final v_x distribution over the whole wing is shown in Fig. 5. It may be noticed how this varies continuously spanwise from the symmetrical picture at $\eta=\infty$ to a completely asymmetrical one at $\eta=0$ (kink section). The maximum supervelocity is located farther back, and its numerical value is much higher than that obtained by Ludwieg. By introducing the function

$$G(\xi)=1-\tfrac{1}{2}\xi \log_e\left(\frac{1+\xi}{1-\xi}\,\frac{1+\sin\varphi}{1-\sin\varphi}\right), \quad . \quad . \quad . \quad (19)$$

the total velocity at the kink section may be represented by

$$|V|=U(1+\delta G\cos\varphi), \quad . \quad . \quad . \quad . \quad . \quad (20)$$

and its maximum by

$$|V|_{max}=U(1+\delta G_{max}\cos\varphi). \quad . \quad . \quad . \quad . \quad (21)$$

The factor G_{max}, which depends on φ, shows the difference between Ludwieg's result and the present one.

The isobars on the swept-back wing of infinite aspect ratio are shown in Fig. 6. The kink effect can be seen clearly, and at some distance from the kink the isobars become almost parallel to the edges, the conditions gradually becoming identical with those on an infinite sheared wing.

Figure 7 shows the function G for different angles of sweepback, and Fig. 8 the product $G\cos\varphi$. The kink effect increases rapidly with φ, but the final effect of sweepback is favourable, though less than that estimated by Ludwieg. Fig. 9 shows this more clearly, the curve $\cos\varphi$ corresponding to Ludwieg's estimate. G_{max} shows the error, and $G_{max}\cos\varphi$ the true effect of sweepback in the danger section.

The results above are limited in their application as they are confined to the bi-convex parabolic profile, which is never used in practice, but they can quite easily be generalised for arbitrary profiles, particularly as regards the kink section. The general formula is as follows

$$(v_x)_{kink}=\left\{(v_x)_{\varphi=0}-\frac{U}{\pi}F'(x)\log_e\frac{1+\sin\varphi}{1-\sin\varphi}\right\}\cos\varphi, \quad . \quad . \quad (22)$$

where $F'(x)$ denotes the first derivative of the equation of the section. The velocity distribution at the kink may therefore be determined immediately from that of the

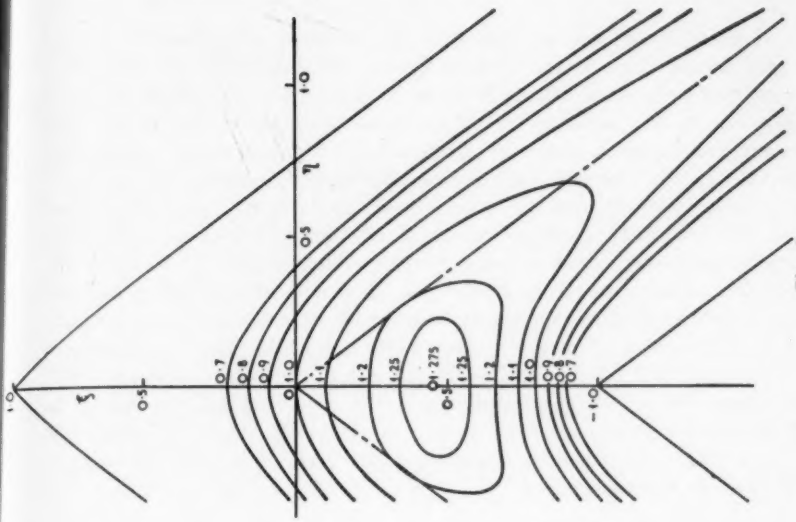

Fig. 6.
Isobars on a swept-back wing. $\varphi = 53° 8'$.

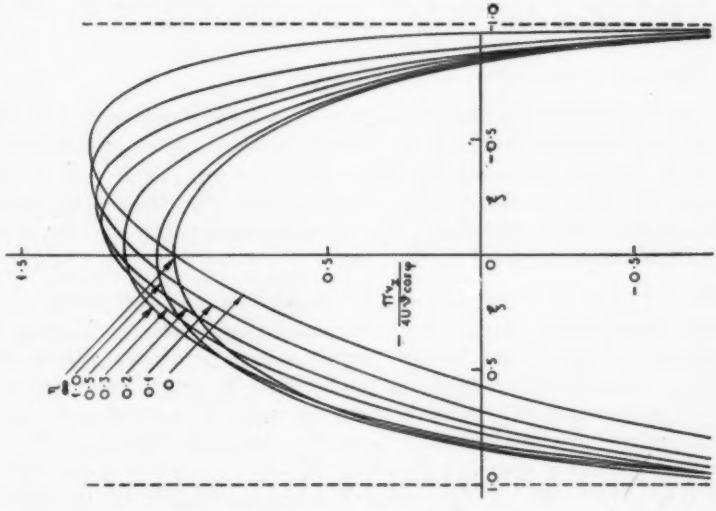

Fig. 5.
v_x distribution over a swept-back wing with bi-convex parabolic section. $\varphi = 53° 8'$.

given section in two-dimensional flow. An example is given in Fig. 10 for a round-nosed profile.

The series of figures which follow show the results of similar calculations for various plan forms. Figs. 11 and 12 show the velocity distribution and the isobars on an *untapered swept-back wing of finite aspect ratio.* The kink effect is seen to be almost exactly the same as in the previous case, but in this case a new phenomenon, the tip effect, makes its appearance. There is a strong tendency for the supervelocities to decrease towards the tips, while the position of the local maximum moves forward and the isobars bend near the tips to become almost parallel to the flow. This seems to indicate that at zero incidence the tips are the least prone to shock-stalling. A warning, however, is now necessary. As mentioned previously, the accuracy of the method is not adequate within a narrow marginal strip, and therefore complete agreement between theory and experiment is hardly to be expected very near to the tips. This tip effect may well prove troublesome in the future, especially if the tips are square-cut or provided with end-plates. With large end-plates, the tip velocity distribution would be quite similar to that at the kink, but reversed fore and aft. For well-rounded tips the results presented here should be a good approximation, although really accurate results can only be obtained by more refined methods.

The interesting point is that, even with the small aspect ratio assumed ($A=2$), the isobars run almost parallel to the edges over a large part of the wing and the velocity field is almost the same as on an infinite sheared wing. For determining critical Mach numbers for wings of fairly large aspect ratio, only two types of section need be considered:

(*i*) The kink section, which is the first danger zone.

(*ii*) The "quasi-two-dimensional" section, *i.e.* a section representative of the large area where conditions are similar to those on an infinite sheared wing, and may therefore be examined on the basis of two-dimensional theory. When critical conditions appear here, the entire wing may be considered as shock-stalled. This point is considered in the second part of this paper.

Figures 13 and 14 show the velocity distribution and the isobars on a *semi-infinite sheared wing,* which is a particularly simple case for studying the isolated tip effect. Figs. 15 and 16 show similar pictures for a *finite sheared wing.* One point in connection with these last figures may be noted. The maximum supervelocity in the centre of a finite sheared wing might be expected to be slightly smaller than on an infinite sheared wing, due to the cutting off of the infinite "tails," carrying their systems of sources and sinks. However, it can be shown that, if $\sin\varphi > 1/\sqrt{3}$, or $\varphi > 35°\ 16'$, the effect is opposite because of the peculiar disposition of sources and sinks. This is shown by the number 1.047 in Fig. 16,

Fig. 7.
Graphs of the function $G(\xi, \varphi)$ for different sweepback angles.

Fig. 8.
Graphs of the function $G(\xi, \varphi)\cos\varphi$ for different sweepback angles.

Fig. 9.
Maximum supervelocity against angle of sweepback.

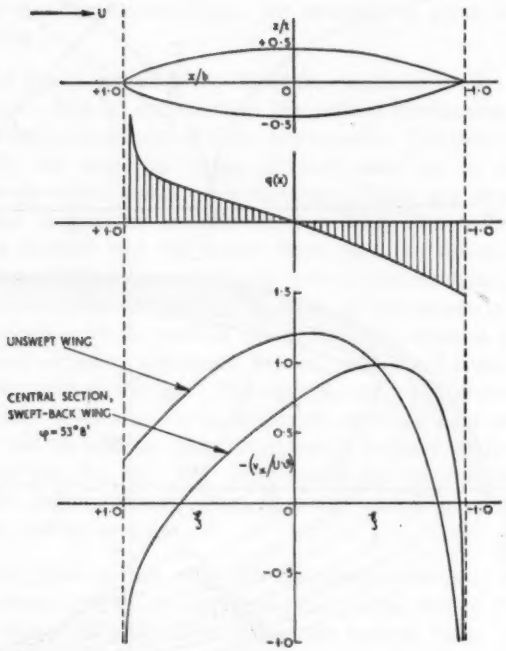

Fig. 10.
Round-nosed profile, sources and supervelocity distribution.

which means that the maximum supervelocity exceeds by 4.7 per cent. that obtained for an infinite sheared wing. This surprising effect is shown in more detail in Fig. 17.

There is a very similar effect of the finite aspect ratio of swept-back wings on the maximum supervelocity in the kink section. An approximate formula, which is sufficiently accurate if the aspect ratio A is not too small, is

$$v_x=(v_x)_{A=\infty}-\frac{4U\vartheta\nu}{\pi A^2}(3\sin^2\varphi-1)\cos^3\varphi, \quad . \quad . \quad . \quad (23)$$

where ν denotes the ratio of the profile area to that of a circumscribed rectangle. The effect may usually be neglected.

In the case of a *tapered wing*, there are further serious difficulties. First, the integrals involved become increasingly complicated and can no longer be reduced to elementary or tabulated types. Second, the number of parameters involved increases alarmingly (angle of sweepback φ_0, coefficient of convergence ε, and taper

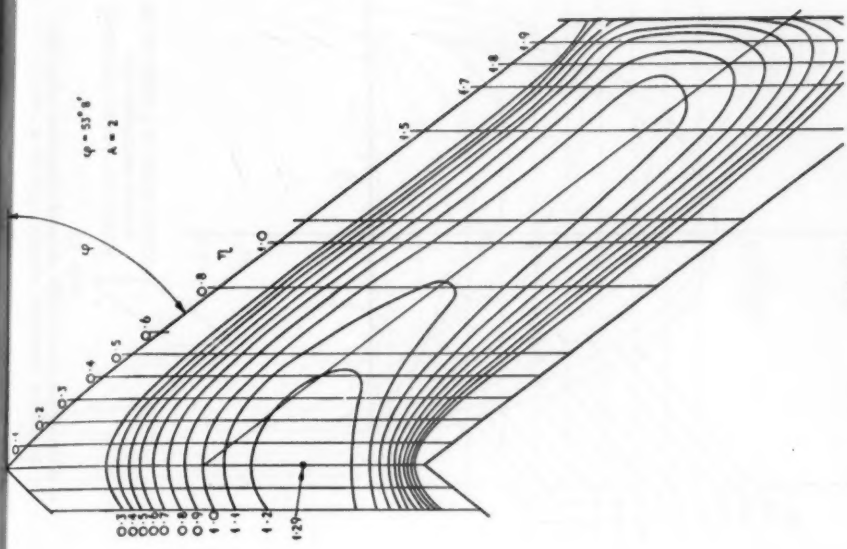

Fig. 12.
Isobars on a finite swept-back untapered wing with bi-convex parabolic section.

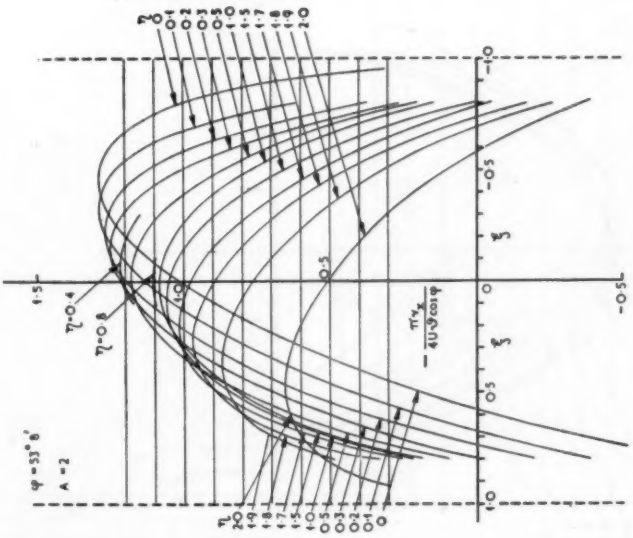

Fig. 11.
v_x distribution over a finite swept-back untapered wing with bi-convex parabolic section.

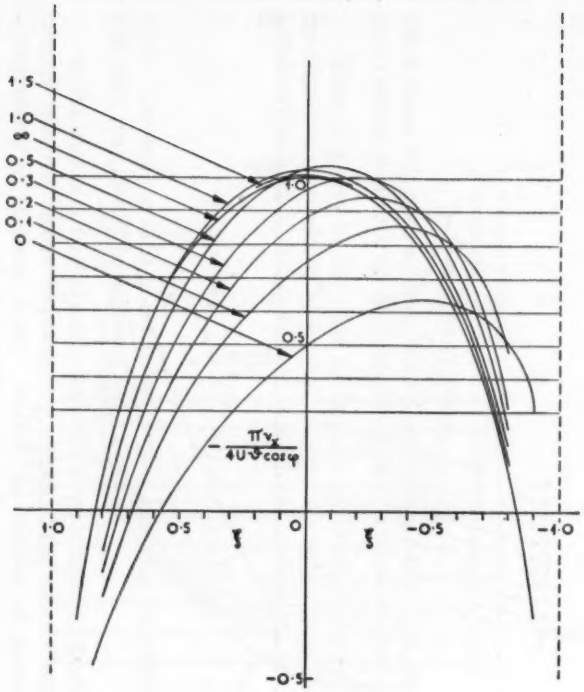

Fig. 13.
v_x distribution over a semi-finite sheared wing with bi-convex parabolic section. $\varphi = 53° 8'$.

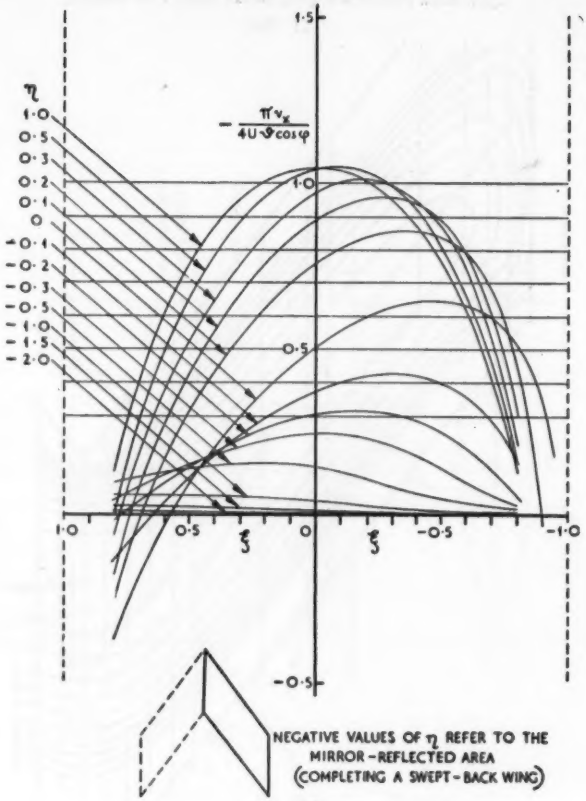

Fig. 15.
v_x distribution over a finite sheared untapered wing with bi-convex parabolic section. $\varphi = 53° 8'$, $A = 2$.

bi-convex parabolic section. $\varphi = 53° 8'$.

γ_1 distribution over a finite sheared untapered wing with bi-convex parabolic section. $\varphi = 53° 8'$, $A = 2$.

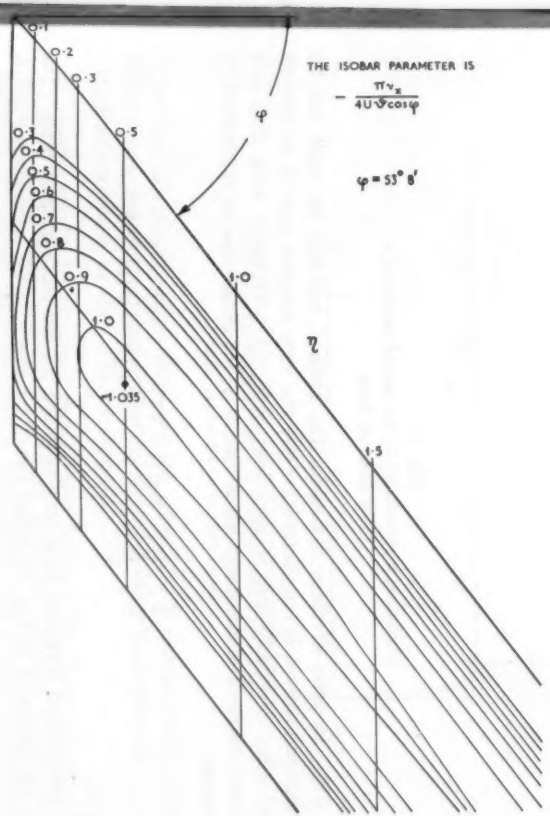

Fig. 14.
Isobars on a semi-infinite sheared wing with bi-convex parabolic section.

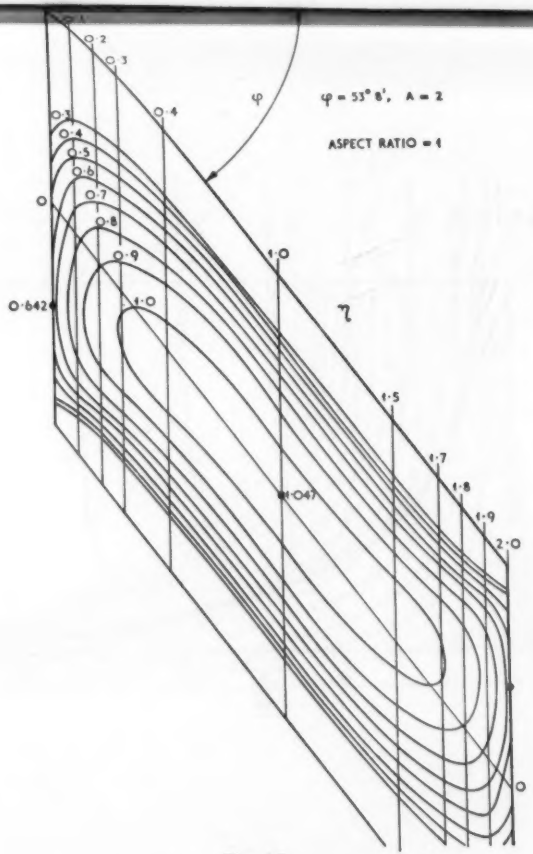

Fig. 16.
Isobars on a finite sheared untapered wing with bi-convex parabolic section.

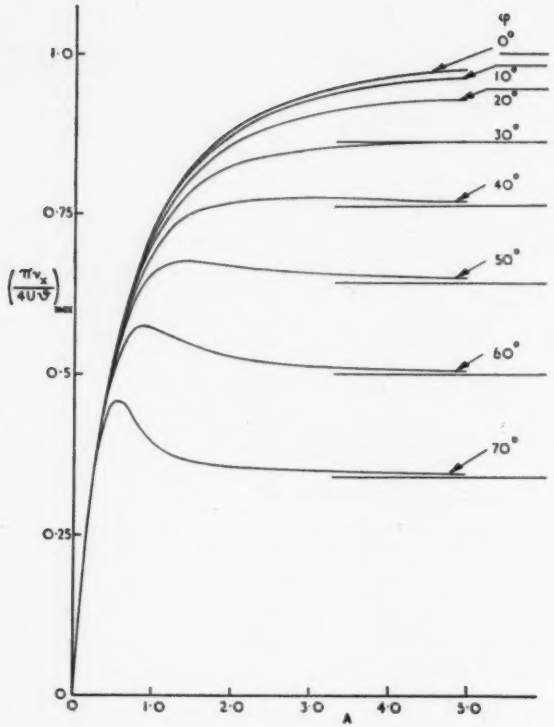

Fig. 17.
Maximum supervelocity in the central section of a finite sheared wing.

ratio ψ†). In spite of these difficulties the method can still be used, but the computation involved is considerable. Only the very simplest case of an unswept tapered wing, especially that of zero taper ratio, *i.e.* a rhombus wing (Fig. 2) is considered here. The maximum supervelocity at the centre can be represented by the formula

$$|v_x|_{\max} = \frac{4}{\pi} U\vartheta \int_0^1 \left[1 + \frac{\log_e (1-Y)}{Y}\right] \frac{dY}{\sqrt{[Y^2 + \varepsilon^2 (1-Y)^2]}}. \qquad (24)$$

$(Y = y/s)$.

More complicated formulae have been obtained for the more general cases. The results are illustrated in Fig. 18, which shows the effects of the parameters ε and ψ.

†Or, alternatively, φ_0, ψ and A (aspect ratio); the parameters used in the text are more convenient.

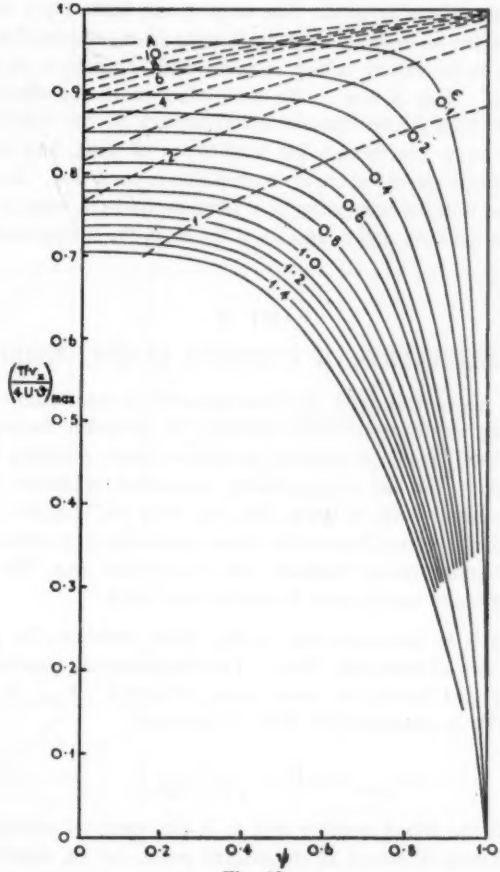

Fig. 18.
Variation of maximum supervelocity of straight tapered wing (at mid-point of central section) with taper ratio ψ and coefficient of convergence ϵ; curves of constant aspect ratio A shown as broken lines.

The effect of ϵ is surprisingly large, but the effect of ψ is comparatively insignificant until ψ becomes quite large. However, large values of ψ correspond to absurdly small aspect ratios, as shown in the diagram.

Similar results for the most general plan form of Fig. 3 are not yet complete, and to represent them adequately a whole series of diagrams would be needed. However, the results presented give a fairly good idea of the significance of the various shape parameters.

One further point is of interest. The drag of any finite body in potential flow is always zero, but for an infinite swept-back wing or a semi-infinite sheared wing, the total drag has finite values, which increase with φ up to a certain maximum, and then fall again. This is due to the kink effect or to the effect of an oblique tip, both of which destroy the fore-and-aft symmetry of the velocity distribution. Fig. 19 shows the drag distribution for both types of wing, and it is remarkable that the total drag (area under the curve) is the same in each case. In this connection it may be remarked that the total drag of a finite swept-back wing is zero, although local drag exists in the kink region and local thrust in the tip regions.

PART II

DETERMINATION OF CRITICAL MACH NUMBERS

Part I of this paper dealt with the determination of maximum velocities, either for the entire wing or for particular sections, in potential incompressible flow. The purpose of Part II is the evaluation of critical Mach numbers, and the results of Part I are used to find the corresponding maximum velocities in compressible flow. There are several ways of doing this, but only the simplest Glauert-Prandtl method, with Göthert's generalisation for three-dimensional problems, is used here. More refined and more recent methods can be applied (*e.g.* the Kármán-Tsien method) but they require much more computational work.

The first step is to determine the critical Mach numbers for any given wing profile in *simple two-dimensional flow*. The fundamental condition is that the maximum velocity just equals the local speed of sound. V_{max} in incompressible flow is given by (9); in compressible flow, it becomes

$$V_{c,\,max} = U\left(1+\frac{\delta}{\sqrt{(1-M^2)}}\right). \quad . \quad . \quad . \quad . \quad . \quad (25)$$

where $M = U/a_0$ is the Mach number and a_0 is the speed of sound in undisturbed flow. The local speed of sound at the critical point can be determined from the generalised Bernouilli equation as

$$a = U\sqrt{\left(1+\frac{2}{\gamma+1}\,\frac{1-M^2}{M^2}\right)}. \quad . \quad . \quad . \quad . \quad . \quad (26)$$

Equating (25) and (26), gives the fundamental relationship

$$\delta = \sqrt{(1-M^2)}\left\{\sqrt{\left(1+\frac{2}{\gamma+1}\,\frac{1-M^2}{M^2}\right)}-1\right\} \quad . \quad . \quad . \quad (27)$$

between maximum supervelocity ratio and critical Mach number in two-dimensional flow. This relationship is represented in Fig. 20 over a large range of δ. The range of practical importance is between $\delta = 0.05$ and 0.2, and in this interval the derivative $dM/d\delta$ differs little from unity. A rough mnemotechnic rule follows that a reduction

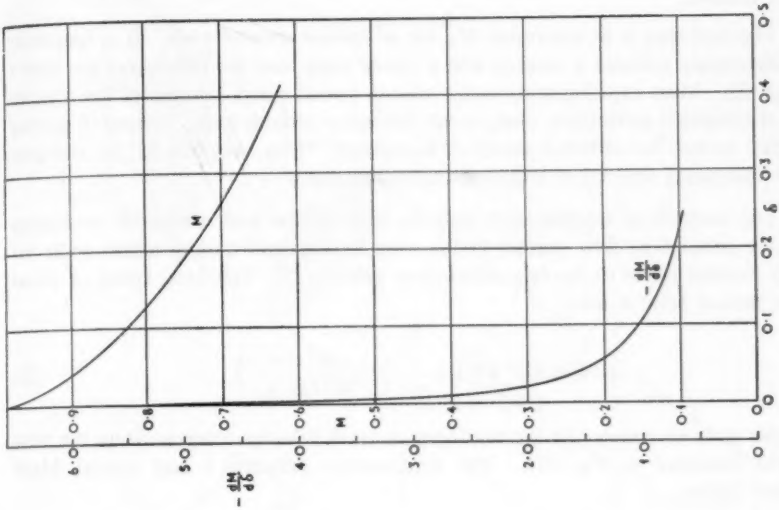

Fig. 20.
Critical Mach number for a straight infinite wing (two-dimensional flow) against maximum supervelocity ratio δ.

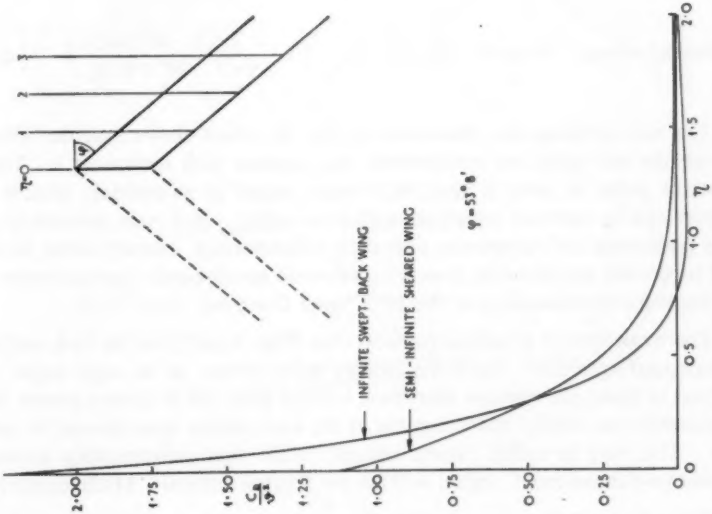

Fig. 19.
Drag distribution over an infinite swept-back or semi-infinite sheared wing.

of $0.01U$ in maximum supervelocity gives an increment of about 0.01 in critical Mach number.

The next step is to determine M_{cr} for an *infinite sheared wing*. It is important to differentiate between a sheared and a *yawed wing*, and the differences are shown in Fig. 21. Most experimental results refer to yawed wings because of the obvious ease of rotating a model in a wind tunnel through a suitable angle, instead of making separate models for different angles of sweepback. This has often led to confusion when comparing theoretical and experimental results.

The methods of treating each case are very similar and consist of considering only the component flow normal to the wing leading and trailing edges, while the Mach number refers to the full undisturbed velocity U. The local speed of sound at the critical point is now

$$a = U\cos\varphi\sqrt{\left(1+\frac{2}{\gamma+1}\,\frac{1-M^2\cos^2\varphi}{M^2\cos^2\varphi}\right)}, \quad . \quad . \quad . \quad (28)$$

and this must be equated to the maximum normal velocity component on the wing (*cf.* the formulae in Fig. 21). The relationships between δ and critical Mach number follow.

For yawed wings: $$\delta = \sqrt{(1-M^2\cos^2\varphi)}\left\{\sqrt{\left(1+\frac{2}{\gamma+1}\,\frac{1-M^2\cos^2\varphi}{M^2\cos^2\varphi}\right)}-1\right\}, \quad . \quad . \quad . \quad . \quad . \quad . \quad . \quad (29)$$

for sheared wings: $$\delta = \sqrt{(1-M^2\cos^2\varphi)}\left\{\sqrt{\left(1+\frac{2}{\gamma+1}\,\frac{1-M^2\cos^2\varphi}{M^2\cos^2\varphi}\right)}-1\right\}\cos\varphi. \quad . \quad . \quad . \quad . \quad . \quad . \quad . \quad (30)$$

The two formulae are illustrated in Fig. 22 which shows that the differences between the two cases are considerable and increase with increasing δ. The most important point to note is that with large angles of sweepback, critical Mach numbers can be obtained which are well above unity. If it were possible to design wings possessing such properties over their entire surface, aircraft would be able to fly at supersonic speeds while preserving subsonic aerodynamic characteristics. This was suggested by Busemann at the 1935 Volta Congress.

The weak spot of a true swept-back wing (Figs. 1 and 3) is the kink section and the surrounding region. Here the isobars must always be at right angles to the direction of flight, the relevant maximum velocity (Fig. 23) is always greater than U, and therefore the critical Mach number at the kink section must always be less than unity. This may be called "lower critical," while that corresponding to the main "quasi-two-dimensional" region will be the "upper critical" Mach number.

The velocity field in compressible flow for a complete swept-back wing can be determined by considering a hypothetical wing ("Göthert's wing") in incompressible

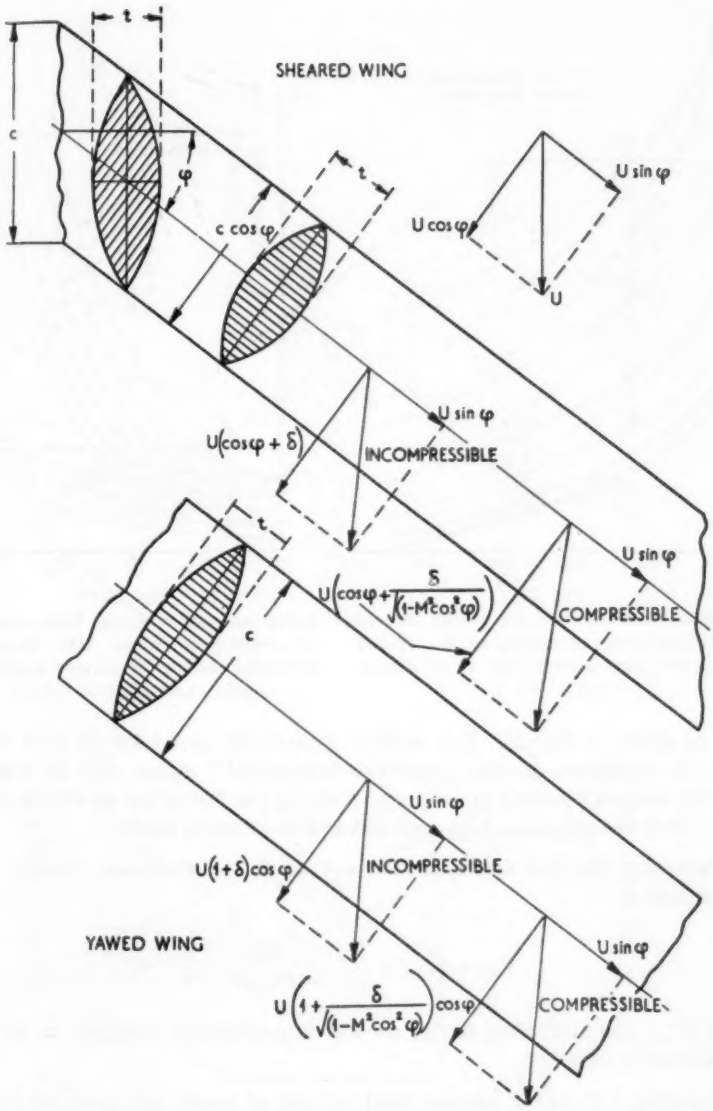

Fig. 21.

Velocity components on infinite sheared or yawed wing, relevant for determining critical Mach number.

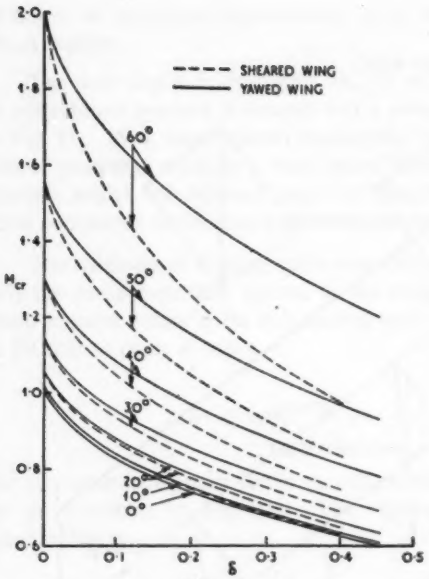

Fig. 22.
Critical Mach numbers for infinite sheared and yawed wings of varying angle φ against maximum supervelocity ratio in two-dimensional flow δ.

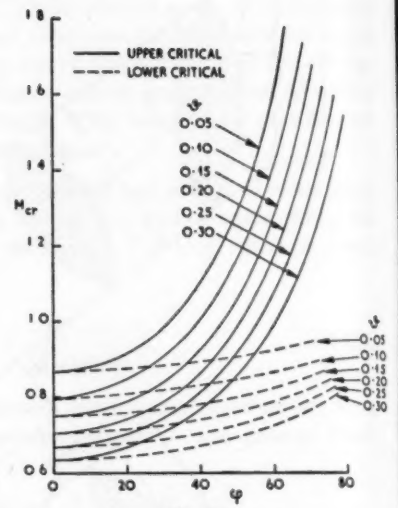

Fig. 24.
Lower and upper critical Mach numbers of swept-back wings with bi-convex parabolic section for varying sweepback angle φ and thickness ratio ϑ.

flow, as shown in Fig. 23. This method is especially useful for the kink section, while the conditions in the "quasi-two-dimensional" region may be examined either by Göthert's method or simply by resolving the flow as for an infinite sheared wing. Both methods have been used and lead to identical results.

Assuming that the aspect ratio is not small, the maximum velocity at the kink section is

$$V_{max}=U\left\{1+\frac{\delta G'_{max}\cos\varphi}{\sqrt{(1-M^2\cos^2\varphi)}}\right\}. \quad . \quad . \quad . \quad (31)$$

where G'_{max} (the kink effect factor, *see* Fig. 9) corresponds expressly to the angle φ' of Göthert's wing.

Equating (31) to the relevant local velocity of sound, still given by (26), we obtain for the lower critical Mach number

$$\delta=\frac{\sqrt{(1-M^2\cos^2\varphi)}}{G'_{max}\cos\varphi}\left\{\sqrt{\left(1+\frac{2}{\gamma+1}\,\frac{1-M^2}{M^2}\right)}-1\right\}. \quad . \quad . \quad (32)$$

Fig. 23.
Velocity components on untapered swept-back wing relevant for determining critical Mach numbers.

This formula can be used only with reference to the particular wing section, because the factor G'_{max} depends on the section shape as well as on φ and M. Fig. 24 shows the results for wings with bi-convex parabolic section, and both the upper and lower critical Mach numbers are shown as functions of sweepback angle φ and thickness ratio ϑ. For large φ, there is a wide gap between the two critical values. When the true Mach number increases from the lower to the upper critical, the supersonic region gradually spreads out from the centre, eventually covering the entire wing. The calculation of the effect of this process on the wave drag is beyond the scope of this paper.

The lower critical Mach number for tapered swept-back wings (particularly delta wings) can be calculated in a similar way, but this requires a great deal of computational work. There is difficulty in defining the upper critical Mach number, since the simple method of resolving the flow into two components cannot be applied directly. The question of what should be considered as the mean or representative angle of sweepback is still an open one.

There are many more problems to be solved in this field, the most important being to extend the theory to cover wings at variable incidence.

ACKNOWLEDGMENT

The author acknowledges the permission of the Chief Scientist, Ministry of Supply, to publish this paper.

REFERENCES

1. GLAUERT, H. (1928). The Effect of Compressibility on the Lift of an Aerofoil. *Proc. Royal Society* A, Vol. 118, 1928.
2. PRANDTL, L. (1930). Über Strömungen, deren Geschwindigkeiten mit der Schallgeschwindigkeit vergleichbar sind. *Journal of the Aeronautical Research Institute, Tokyo Imperial University*, No. 65, 1930.
3. PRANDTL, L. (1935). Allgemeine Betrachtungen über die Strömung zusammendrückbarer Flüssigkeiten. Proceedings of the Volta Congress, Rome 1935. Also *Zeitschrift für Angewandte Mathematik und Mechanik*, June 1936.
4. LUDWIEG, H. (1940). Pfeilflügeln bei hohen Geschwindigkeiten. Bericht 127 der Lilienthal-Gesellschaft, 1940.
5. GÖTHERT, B. (1940). Berechnung des Geschwindingkeitsfeldes von Pfeilflügeln bei hohen Unterschallgeschwindigkeiten. Bericht 127 der Lilienthal-Gesellschaft, 1940.
6. GÖTHERT, B. (1940). Ebene und raümliche Strömung bei hohen Unterschallgeschwindigkeiten (Erweiterung der Prandtlschen Regel). Bericht 127 der Lilienthal-Gesellschaft, 1940.
7. LUDWIEG, H. (1946). Improvement of the Critical Mach Number of Aerofoils by Sweepback. M.A.P. Völkenrode Report. R. & T. 84. GDC 10/4258 T.
8. LEE, G. H. (1947). Tailless Aircraft Design Problems. *Journal of The Royal Aeronautical Society*, February 1947, pp. 121 *et seq.*
9. RICHARDS, E. J. (1948). Practical Design Problems Arising from Sweepback. Anglo-American Aeronautical Conference, London, 3rd-5th September, 1947, *Aeronautical Conference*, 1948, pp. 382, 400.

GENERAL PERFORMANCE REDUCTION EQUATIONS FOR RECIPROCATING-ENGINED AIRCRAFT WITH CONSTANT-SPEED PROPELLERS

by

W. J. D. ANNAND, B.Sc., A.F.R.Ae.S.
(Rolls-Royce Limited, Hucknall)

SUMMARY

The method of analysis adopted by Cameron[1] has been extended to develop more general equations for the correction of level speed and rate of climb for variation of air temperature and aircraft weight, applicable to aircraft with reciprocating engines of any type driving constant-speed propellers, operating at speeds sufficiently high for compressibility effects on drag and propeller efficiency to be appreciable. Allowance is made in the equations for ram effect on engine power.

The practical application of the equations is discussed, and illustrated by a worked example. The influence of errors in the estimation of the parameters expressing the variation of engine power and propeller efficiency on the corrections, in this particular case, is discussed.

1. INTRODUCTION

In order that measurements of the performance of an aircraft made at different times may be correlated and compared, it is necessary to have a method of determining or eliminating the effects of variation of those parameters which cannot be held constant. This process is called "performance reduction." In what are known as "analytical" methods of performance reduction, the variation of performance with the uncontrolled parameters is determined explicitly, and the observed performance is reduced to standard values of the parameters by the numerical correction of individual observations. In practice, the uncontrolled parameters are most commonly the air temperature and the weight of the aircraft.

Analytical methods of performance reduction for piston-engined aircraft with constant-speed propellers, operating at Mach numbers below the critical value for drag rise, were developed in 1942 by Cameron[1]. The working methods set out in that reference are in general use at the present time. Their application, however, is limited by the purposes for which they were developed: they were intended to

Paper received November 1949.
[The Aeronautical Quarterly, Vol. II, August 1950]

yield approximately correct results for all types of aircraft falling within the above category, and for this purpose certain simplifications were adopted and average numerical values of certain parameters were employed.

In the present paper, the author has followed the general line of approach adopted by Cameron, to develop more general equations for the correction of level speed and rate of climb for variations of air temperature and of aircraft weight, at constant air pressure and propeller r.p.m. The equations given include allowances for the effect of compressibility on aircraft drag and on propeller efficiency, and for the effect of ram on engine power. They are developed in a form such that they may be applied to aircraft powered by any type of reciprocating engine driving a constant-speed propeller.

As neither Cameron's paper, nor any other on analytical methods of performance reduction, has yet been published, to the author's knowledge, the derivation of the equations is given in detail, in the belief that the indication of the methods of attack applicable to this and similar problems will be of value to students.

Notation

A	aspect ratio of wing
b	span of wing
C	engine supercharger constant
C_D	total drag coefficient
C_{Dz}	$C_D - KC_L^2/(\pi A)$
C_{Dz0}	value of C_{Dz} at low Mach number
C_L	lift coefficient
C_p	propeller power coefficient
c	engine cylinder compression ratio
D	total drag of aircraft
d	propeller diameter
E_J	propeller parameter $= (J/\eta)\,\partial\eta/\partial J$
E_M	propeller parameter $= (M_t/\eta)\,\partial\eta/\partial M_t$
E_P	propeller parameter $= (C_p/\eta)\,\partial\eta/\partial C_p$
F	$P_1 - P$
$f(m, M)$	$[m^4(\alpha\mu + 3\alpha - 1)] / [\alpha m^4 + 1]$
J	propeller advance coefficient $= V_1/(nd\sqrt{\sigma})$
K	(πA) times the slope of the curve of C_D against C_L^2 at constant Mach number

M Mach number

M_t propeller tip Mach number

m V_i/V_{imd}

n propeller rotational speed

P power delivered to propeller shaft

P_i indicated power of engine (*i.e.* power developed in cylinder)

p ambient air pressure

p_i stagnation pressure of air in engine intake

S wing area

T_i stagnation temperature of air in engine intake

t ambient air temperature

t_s standard value of air temperature to which the performance is to be corrected

V_i equivalent air speed = (true air speed) $\times \sqrt{\sigma}$

V_{imd} equivalent air speed for minimum drag at low altitude

$$= \left(\frac{4KW^2}{\pi\rho_0^2 Sb^2 C_{DZ0}}\right)^{0.25}$$

v_c true (tape-measure) rate of climb

v_{cs} value of v_c corrected to the I.C.A.N. standard temperature at the test height

v_{cp} rate of climb indicated by an altimeter calibrated according to the I.C.A.N. convention

W weight of aircraft

Y $\frac{1}{2}\rho_0 S C_{DZ0}$

Z $K/(\frac{1}{2}\pi\rho_0 b^2)$

z engine parameter, depending on the rotational speed, representing the charge temperature rise from intake to cylinder

Δt deviation of temperature from standard $= t - t_s$

ΔW deviation of weight from standard

ΔV_i correction to be added to observed V_i to obtain the value at the standard temperature or weight

Δv_c correction to be added to observed v_c to obtain the value at the standard temperature or weight

α C_{DZ}/C_{DZ0}

β M/M_t

γ ratio of the specific heat of air at constant pressure to that at constant volume

η	propeller efficiency
η_i	air intake efficiency
μ	$(M/C_{DZ})dC_{DZ}/dM$
Π_t	$(t/P)\partial P/\partial t$
Π_V	$(V_i/P)\partial P/\partial V_i$
ρ	air density
ρ_0	standard value of air density at sea level
σ	ρ/ρ_0
ϕ	$2\Pi_t(1+E_P)+E_J+2E_P-(1-\beta)E_M-1$

2. ASSUMPTIONS MADE

The following basic assumptions are made:

(*i*) The drag coefficient C_D of the aircraft may be expressed as the sum of two parts, one of which, C_{DZ}, is independent of C_L, and the other of which is proportional to C_L^2. In the usual notation,

$$C_D = C_{DZ} + \frac{K}{\pi A} C_L^2.$$

This assumption is that generally employed in performance calculations. It is known to be inexact at high C_L, but is considered to be sufficiently accurate for the calculation of small performance changes, throughout the normal flight range of speeds.

(*ii*) Only the part C_{DZ} of the total drag varies with Mach number. Evidence as to the variation of K is scanty and, for the present, the additional complication introduced by allowing for such variation does not appear justified. It is convenient to write $C_{DZ} = \alpha\, C_{DZ_0}$ where C_{DZ_0} is the value of C_{DZ} at low (nominally zero) Mach number.

(*iii*) The power P delivered to the propeller shaft is a function only of the air pressure p, the air temperature t, and the equivalent air speed V_i. The inclusion of V_i in the parameters allows for the effect on the engine power of the ram pressure and temperature rises in the air intake of the engine.

(*iv*) The propeller efficiency η is a function only of the advance ratio J, the power coefficient C_p, and the tip Mach number M_t.

(*v*) No thrust is obtained from the exhaust gases. This assumption is made to avoid excessive complication in the analysis. A method of estimating the effect of variation of exhaust thrust, and some indication of the magnitude of this effect, are given in Ref. 2.

3. BASIC EQUATIONS

Using assumptions (*i*), (*ii*) and (*v*), the well-known performance equation is obtained

$$\eta P\sqrt{\sigma}=\tfrac{1}{2}\rho_0 S\alpha C_{D_{20}}V_1^3+KW^2/(\tfrac{1}{2}\pi\rho_0 b^2V_1)+Wv_c\sqrt{\sigma}.$$

To simplify manipulation this is written in the form

$$\eta P\sqrt{\sigma}=Y\alpha V_1^3+ZW^2/V_1+Wv_c\sqrt{\sigma} \quad . \quad . \quad . \quad . \quad (1)$$

where Y and Z depend only on the aircraft configuration. The total drag of the aircraft is given by

$$D=Y\alpha V_1^3+ZW^2/V_1^2,$$

whence is obtained the equivalent air speed at which the drag would be a minimum if no compressibility effects existed,

$$V_{ind}=(ZW^2/Y)^{0.25}$$

$$=\left(\frac{4KW^2}{\pi\rho_0^2Sb^2C_{D_{20}}}\right)^{0.25}$$

At constant air pressure and engine r.p.m. the following relations hold:

$$\frac{1}{\eta}\frac{\partial\eta}{\partial t}=\left(\frac{J}{\eta}\frac{\partial\eta}{\partial J}\right)\left(\frac{1}{J}\frac{\partial J}{\partial t}\right)+\left(\frac{C_p}{\eta}\frac{\partial\eta}{\partial C_p}\right)\left(\frac{1}{C_p}\frac{\partial C_p}{\partial t}\right)+\left(\frac{M_t}{\eta}\frac{\partial\eta}{\partial M_t}\right)\left(\frac{1}{M_t}\frac{\partial M_t}{\partial t}\right)$$

$$=E_J\left(-\frac{1}{2\sigma}\frac{\partial\sigma}{\partial t}\right)+E_P\left(\frac{1}{P}\frac{\partial P}{\partial t}-\frac{1}{\sigma}\frac{\partial\sigma}{\partial t}\right)+E_M\left(-\frac{1-\beta}{2t}\right)$$

$$=\frac{1}{2t}[E_J+2E_P(1+\Pi_t)-(1-\beta)E_M]$$

$$\frac{1}{\eta}\frac{\partial\eta}{\partial V_1}=\frac{1}{V_1}[E_J+E_P\Pi_V+\beta E_M]$$

$$\frac{d\alpha}{dt}=\left(\frac{M}{\alpha}\frac{d\alpha}{dM}\right)\alpha\left(\frac{1}{M}\frac{dM}{dt}\right)$$

$$=\frac{\alpha\mu}{V_1}\frac{dV_1}{dt}.$$

4. VARIATION OF PERFORMANCE WITH TEMPERATURE AND WEIGHT AT CONSTANT PRESSURE AND ENGINE R.P.M.

4.1. *Variation of speed in level flight with temperature*

Putting $v_c=0$ in equation (1) and differentiating with respect to temperature at constant weight,

$$\frac{1}{\eta}\frac{d\eta}{dt}+\frac{1}{P}\frac{dP}{dt}+\frac{1}{\sqrt{\sigma}}\frac{d\sqrt{\sigma}}{dt}=\frac{YV_i^3\frac{d\alpha}{dt}+3Y\alpha V_i^2\frac{dV_i}{dt}-\frac{ZW^2}{V_i^2}\frac{dV_i}{dt}}{Y\alpha V_i^3+ZW^2/V_i}.$$

Substituting from the relations given in Section 3,

$$\frac{1}{V_i}\frac{dV_i}{dt}[E_J+E_P\Pi_Y+\beta E_M]+\frac{1}{2t}[E_J+2E_P(1+\Pi_t)-(1-\beta)E_M]+\frac{\Pi_t}{t}+$$

$$+\frac{1}{V_i}\frac{dV_i}{dt}\Pi_Y-\frac{1}{2t}=\frac{\left[\frac{Y}{ZW^2}V_i^4(\alpha\mu+3\alpha)-1\right]\frac{1}{V_i}\frac{dV_i}{dt}}{\frac{Y}{ZW^2}V_i^4\alpha+1}$$

$$=\left[\frac{m^4(\alpha\mu+3\alpha)-1}{\alpha m^4+1}\right]\frac{1}{V_i}\frac{dV_i}{dt},$$

which gives on re-arrangement,

$$\frac{t}{V_i}\frac{dV_i}{dt}=\frac{\frac{1}{2}[2\Pi_t(1+E_P)+E_J+2E_P-(1-\beta)E_M-1]}{f(m,M)-(E_J+\beta E_M)-\Pi_Y(1+E_P)}.$$

4.2. *Variation of speed in level flight with weight*

Similarly, by differentiation at constant temperature,

$$\frac{1}{\eta}\frac{\partial\eta}{\partial V_i}\frac{dV_i}{dW}+\frac{1}{P}\frac{\partial P}{\partial V_i}\frac{dV_i}{dW}=\frac{YV_i^3\frac{d\alpha}{dV_i}\frac{dV_i}{dW}+3Y\alpha V_i^2\frac{dV_i}{dW}-\frac{ZW^2}{V_i^2}\frac{dV_i}{dW}+\frac{2ZW}{V_i}}{Y\alpha V_i^3+ZW^2/V_i},$$

which gives, on substitution,

$$\frac{1}{V_i}\frac{dV_i}{dW}(E_J+E_P\Pi_Y+\beta E_M+\Pi_Y)=\frac{\left[\frac{Y}{ZW^2}V_i^4(\alpha\mu+3\alpha)-1\right]\frac{1}{V_i}\frac{dV_i}{dW}+\frac{2}{W}}{\frac{Y}{ZW^2}V_i^4\alpha+1}$$

and on re-arrangement

$$\frac{W}{V_i}\frac{dV_i}{dW} = \frac{-2}{(\alpha m^4+1)[f(m,M)-(E_J+\beta E_M)-\Pi_Y(1+E_P)]}.$$

4.3. *Variation of rate of climb with temperature at constant* V_i

Differentiating equation (1) at constant V_i,

$$\frac{1}{\eta}\frac{\partial\eta}{\partial t}+\frac{1}{P}\frac{\partial P}{\partial t}+\frac{1}{\sqrt{\sigma}}\frac{d\sqrt{\sigma}}{dt} = \frac{W\sqrt{\sigma}\dfrac{dv_c}{dt}+Wv_c\dfrac{d\sqrt{\sigma}}{dt}}{Y\alpha V_i^3+ZW^2/V_i+Wv_c\sqrt{\sigma}},$$

which gives on substitution

$$\frac{1}{2t}[E_J+2E_P(1+\Pi_t)-(1-\beta)E_M]+\frac{\Pi_t}{t}-\frac{1}{2t} = \frac{\dfrac{dv_c}{dt}-\dfrac{v_c}{2t}}{\dfrac{V_i}{\sqrt{\sigma}}\left(\alpha\dfrac{YZV_i^2}{ZW}+\dfrac{YZW^2}{YV_i^2}\right)+v_c}$$

and therefore

$$\frac{dv_c}{dt} = \frac{v_c}{2t}+\frac{1}{2t}\left[v_c+\frac{V_i}{\sqrt{\sigma}}\left(\frac{KC_{TV^2\theta}}{\pi A}\right)^{0.5}(\alpha m^2+1/m^2)\right]\times$$
$$\times\left[2\Pi_t(1+E_P)+E_J+2E_P-(1-\beta)E_M-1\right]$$

4.4. *Variation of rate of climb with weight at constant* V_i

In this case, differentiation with respect to weight gives

$$0 = 2ZW/V_i+v_c\sqrt{\sigma}+W\sqrt{\sigma}\;dv_c/dW$$

Therefore
$$dv_c/dW = -(1/W)\left[v_c+2ZW/(V_i\sqrt{\sigma})\right]$$

5 WORKING EQUATIONS

From the equations already developed the following working equations can be obtained for the corrections to be added to the observed values of V_i and v_c for deviations Δt and ΔW from the standard values of temperature and weight.

Level flight

$$\frac{\Delta V_i}{V_i} = -\frac{\frac{1}{2}\phi\Delta t/t}{f(m,M)-(E_J+\beta E_M)-\Pi_Y(1+E_P)}. \quad . \quad . \quad . \quad . \quad . \quad (2)$$

$$\frac{\Delta V_i}{V_i} = \frac{2\Delta W/W}{(\alpha m^4+1)[f(m,M)-(E_J+\beta E_M)-\Pi_Y(1+E_P)]} \quad . \quad . \quad . \quad (3)$$

Climb

$$\Delta v_c = -\frac{\Delta t}{2t}\left\{v_c + \phi\left[v_c + \frac{V_i}{\sqrt{\sigma}}\left(\frac{KC_{DZ0}}{\pi A}\right)^{0.5}(\alpha m^2 + 1/m^2)\right]\right\} \quad . \quad . \quad (4)$$

$$\Delta v_c = \frac{\Delta W}{W}\left\{v_c + \frac{4}{\pi\rho_0}\frac{K}{b^2}\frac{W}{V_i\sqrt{\sigma}}\right\} \quad . \quad . \quad . \quad . \quad . \quad . \quad (5)$$

where ϕ represents the sum

$$2\Pi_i(1+E_P)+E_J+2E_P-(1-\beta)E_M-1.$$

It should be noted that ϕ will in general be negative so that ΔV_i is positive for positive $\Delta t = t - t_s$. Note also that in the equations as presented here consistent units are employed.

These equations reduce to those developed by Cameron[1] for $\alpha = 1.0$, $\mu = E_P = E_M = \Pi_V = 0$.

The correction Δv_c given for a temperature deviation Δt is the correction to the true tape-measure rate of climb. Usually, the rate of climb is measured by the variation of the reading of an I.C.A.N.-calibrated altimeter. If a test is made on a day when the temperature is other than the I.C.A.N. standard, the altimeter does not indicate the true rate of climb but gives the variation v_{cp} of the pressure height with time. The relation between v_{cp} and v_c is

$$v_c/v_{cp} = t/t_s \quad . \quad . \quad . \quad . \quad . \quad . \quad (6)$$

where t and t_s are the test and standard temperatures at the pressure height in question. Thus

$$\frac{v_c - v_{cp}}{v_{cp}} = \frac{t - t_s}{t_s} \approx \frac{\Delta t}{t},$$

and the correction to be added to v_{cp} to give the true rate of climb v_{cs} at the standard temperature t_s can be written

$$v_{cs} - v_{cp} \approx \frac{\Delta t}{2t}\left\{v_{cp} - \phi\left[v_{cp} + \frac{V_i}{\sqrt{\sigma}}\left(\frac{KC_{DZ0}}{\pi A}\right)^{0.5}(\alpha m^2 + 1/m^2)\right]\right\},$$

neglecting terms of second order in $\Delta t/t$.

Note that if it is desired to correct the observed rate of climb to conditions other than the I.C.A.N. standard, this last equation cannot be used, and equation (4) must be employed, first correcting all observations to the true rates of climb by (6).

6. PRACTICAL APPLICATION

The dependence of the "compressibility" parameters α, μ and E_M and of the ratio β on the design of the aircraft is such that it is impossible to make use of average values to construct simple general curves from which the corrections might be read off for any aircraft. However, for any given case it is a fairly simple task to construct sets of curves from which the corrections may be read off as functions of equivalent air speed and altitude, on the assumption that the substitution of t_s for t in the correction formulae will not seriously affect the accuracy, so that altitude may be taken to determine both the pressure (which with V_i determines M) and the value to be used for t in the formulae. This assumption is clearly valid for all cases in which the use of a "differential" correction is justified.

The construction of such curves will be illustrated by a numerical example (Section 7), but some general remarks on the derivation of the various parameters may be helpful. The various drag parameters $C_{D_{Z_0}}$, K, α and μ may be obtained from wind tunnel measurements, or by analysis of flight performance measurements. α and μ will be functions of M only. Experience suggests that in general the values of E_J and E_P will vary little with flight condition within a given régime—*i.e.* climb or level flight— and that for a given régime they may be considered to vary linearly with V_i and altitude; thus they need only be calculated for a few limiting conditions. The method of estimation of propeller efficiency recently published by the S.B.A.C.[3] is very suitable for the estimation of all three propeller functions. The values of Π_t and Π_T will usually be fairly easy to obtain, either graphically from test-bed measurements of the response of the engine to variation of intake pressure and temperature, or analytically from formulae for the engine performance when these are available. If assumption (*iii*) holds, Π_T and Π_t also are (with sufficient accuracy) functions of altitude and V_i only. The derivation of formulae for Π_T and Π_t for the conventional four-stroke mechanically supercharged engine is given in Appendix I as an illustration.

7. ILLUSTRATIVE EXAMPLE

As an example of the construction of working charts for a particular case, the corrections to level speed for weight and temperature variations from standard will now be worked out for a hypothetical aircraft, and the influence of certain of the parameters in this case will be discussed. The basic aircraft data are

Wing area $S=200$ ft.^{2}

Wing span $b=35$ ft.

$C_{D_Z}=0.015$

$K=1.20$.

The weight chosen as standard is 10,100 lb., at which V_{imd} is 200 m.p.h.

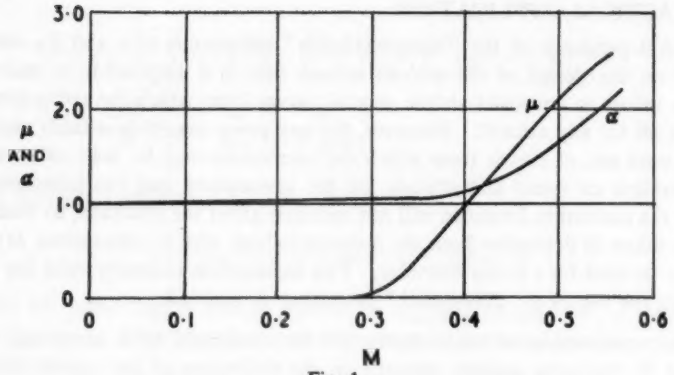

Fig. 1.
Variation of α and μ with M for example aircraft.

In Fig. 1, α and μ are plotted against Mach number. The Mach number at which the drag rise begins has been chosen somewhat lower than would be expected on a well-designed aircraft, in order to illustrate the effect of the drag rise on the corrections.

The maximum Mach number for level flight at sea level has been taken as 0·50. The power required for this performance is 3,500 horse power and the propeller diameter has been chosen to absorb this power according to the recommendations of Ref. 4. The propeller details are

Diameter $d=16$ ft.

Number of blades $=4$

Solidity at 0.7 radius $=0.15$

Thickness/chord ratio $=0.07$ at 0.7 radius
0.20 at root.

The engine parameters are

$$C=0.002$$

$$z=150°.$$

For simplicity, F/P has been taken to be constant at 0.10, and the intake efficiency η_i has been taken to be 0.90. The maximum engine speed is 1,194 r.p.m. at the propeller shaft.

From these data, the values of the engine and propeller parameters have been calculated for sea level and 30,000 ft. altitude, from Appendix I and Ref. 3 respectively. The results are plotted against equivalent air speed in Figs. 2, 3 and 4. The very small variation of E_J and E_P will be observed.

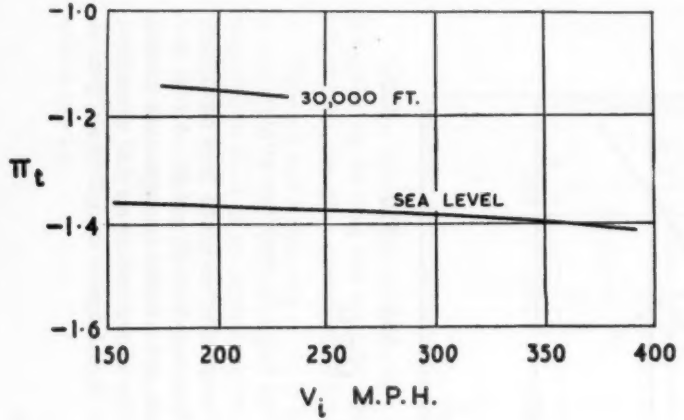

Fig. 2.
Variation of Π_t with V_i for example aircraft at full throttle.

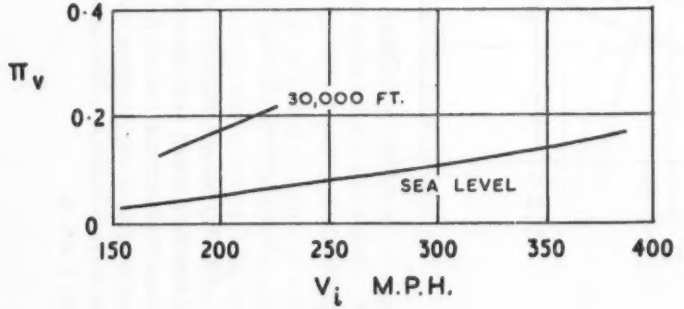

Fig. 3.
Variation of Π_V with V_i for example aircraft at full throttle.

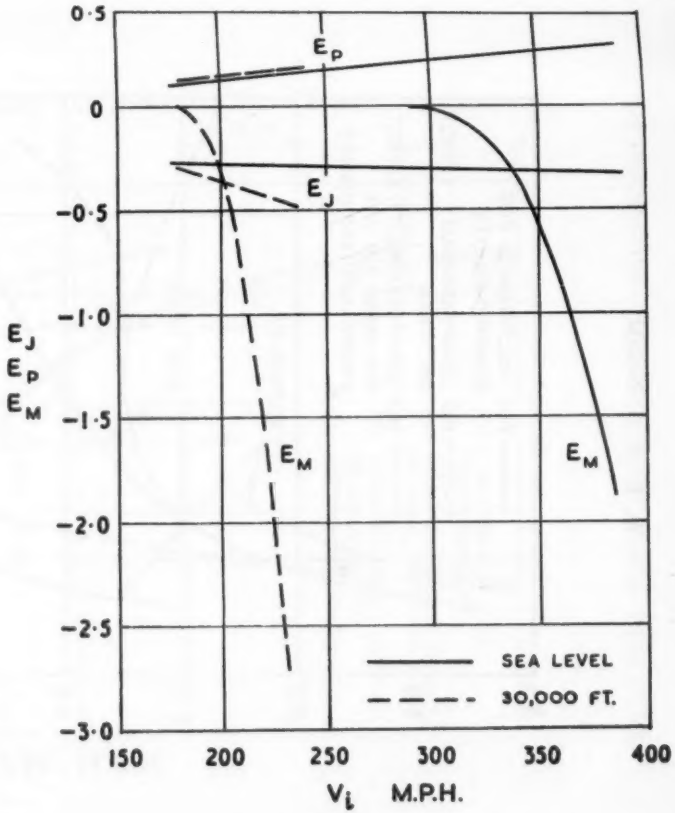

Fig. 4.
Variation of E_J, E_P and E_M with V_i for example aircraft.

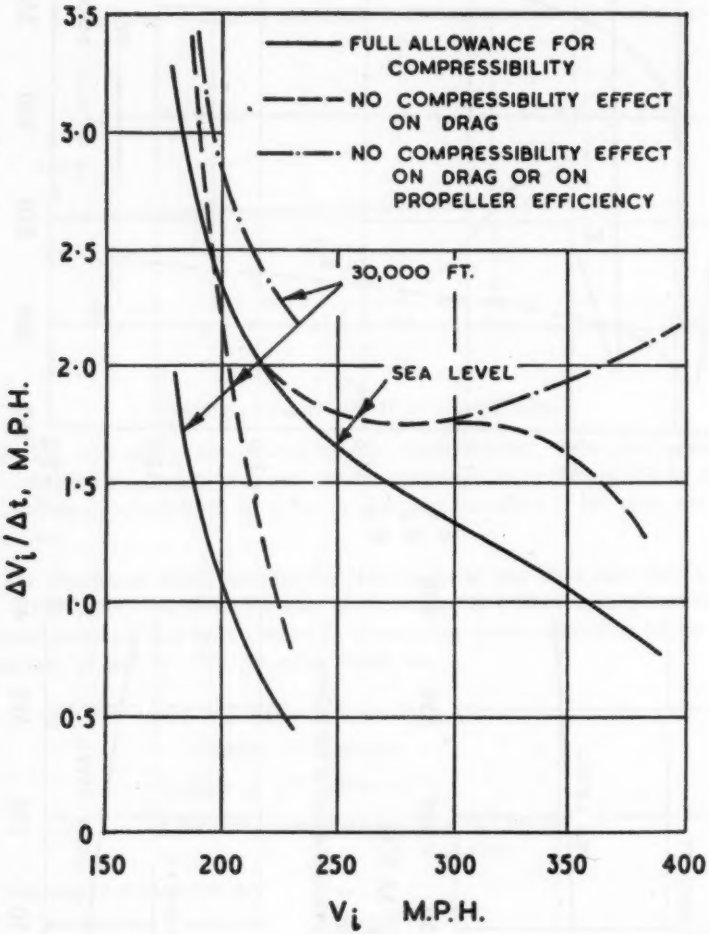

Fig. 5.
Example aircraft. Correction to speed at full throttle for temperature variation.

Finally, the corrections for weight and temperature variations from standard at full throttle opening have been calculated from equations (2) and (3). Values of β for use in these equations have been estimated on reasonable assumptions concerning the variation of engine power with r.p.m.; the average values are 0.47 at sea level and 0.63 at 30,000 ft. The corrections are plotted against equivalent air speed in Figs. 5 and 6.

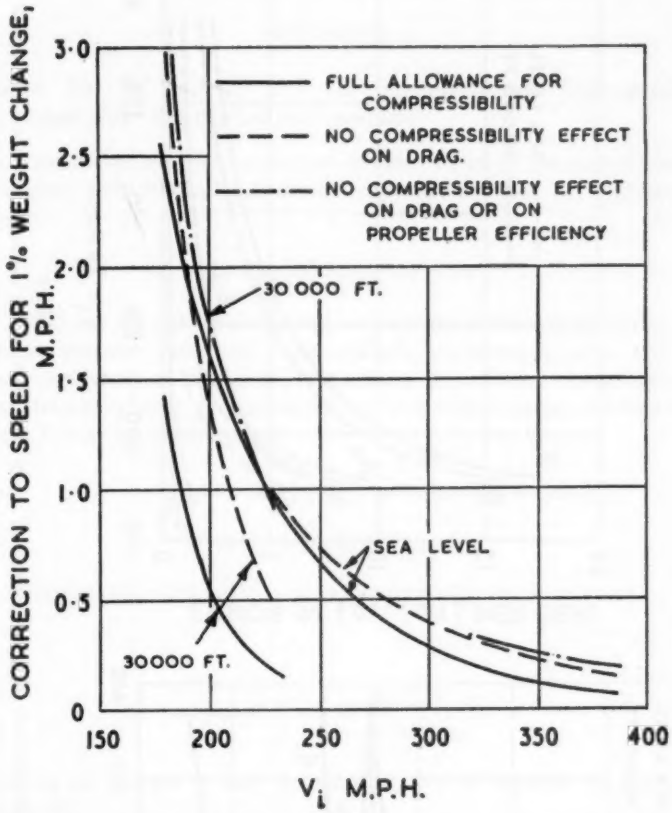

Fig. 6.
Example aircraft—correction to speed at full throttle for weight variation.

In these figures, the curves which would be obtained if the effects of compressibility on the drag and propeller efficiency were neglected are also shown. As will be seen, the effect of compressibility is to reduce the corrections considerably.

Figures 7 and 8 show the errors in the corrections produced by errors of +0.1 in estimation of the various engine and propeller parameters. An error of this magnitude in E_P is of no importance, the resulting error in the correction being less than 2.5 per cent. of the correction at all conditions. At high speeds, the effect of error in Π_t on the temperature correction is by far the greatest (it has of course no effect on the weight correction). The effects of errors in the other parameters vary considerably with speed, and become quite large at low speed; fortunately, in this region Π_F and E_M are usually small, and large errors in their estimation are unlikely to arise.

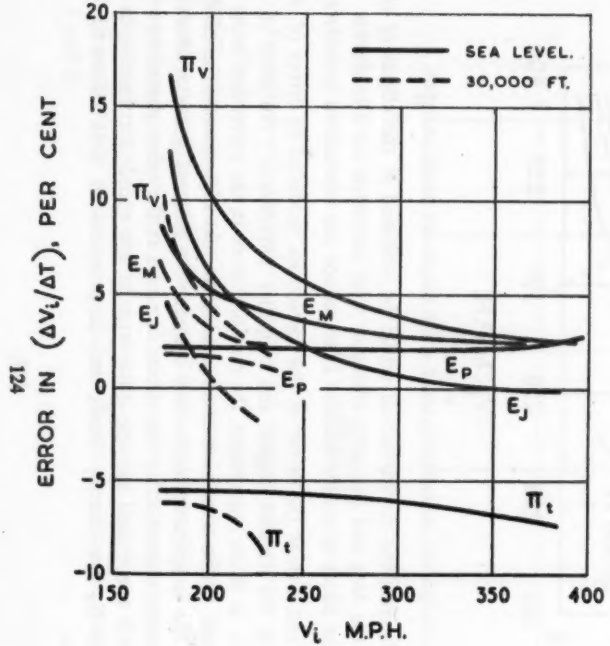

Fig. 7.

Effect of +0.10 error in estimating various parameters on the temperature correction to speed for the example aircraft at full throttle.

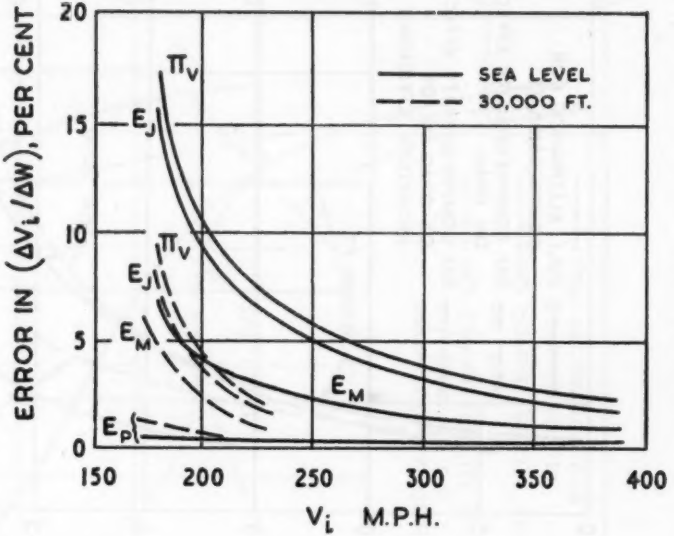

Fig. 8.

Effect of +0.10 error in estimating various parameters on the weight correction to speed for the example aircraft at full throttle.

APPENDIX I

Formulae for Π_t and Π_V for the conventional four-stroke mechanically supercharged engine

It is known that the performance at constant r.p.m. of the conventional four-stroke engine with mechanically-driven supercharger can be represented by the relation:

$$(P+F) \propto (rp_i - p/c)/(T_i + z).$$

Here p_i and T_i are the total pressure and temperature in the engine intake, r is the supercharger pressure ratio and c the cylinder compression ratio, and z is a parameter, dependent on the r.p.m., representing the effective charge temperature rise from intake to cylinder, due to compression in the supercharger and heat transfer. For p_i and T_i may be substituted

$$p_i \approx p(1 + \tfrac{1}{2}\eta_i \gamma M^2) \text{ with sufficient accuracy,}$$

$$T_i = t(1 + \tfrac{1}{2}(\gamma - 1)M^2) \text{ exactly,}$$

where η_i represents the intake efficiency and may be taken to be constant.

Thus

$$(P+F) \propto \frac{p[r(1 + \tfrac{1}{2}\eta_i \gamma M^2) - 1/c]}{t[1 + \tfrac{1}{2}(\gamma - 1)M^2] + z}.$$

Differentiating at constant p, and remembering that at constant V_i and p, M is independent of t,

$$\frac{1}{P+F}\frac{\partial P}{\partial t} = \frac{1}{r - 1/[c(1 + \tfrac{1}{2}\eta_i \gamma M^2)]}\frac{\partial r}{\partial t} - \frac{1 + \tfrac{1}{2}(\gamma - 1)M^2}{t[1 + \tfrac{1}{2}(\gamma - 1)M^2] + z}. \quad . \quad (a)$$

It is generally accepted[1] that the variation of r with temperature at constant engine r.p.m. and throttle opening can be represented by

$$r \propto [1 + (288 - T_i)C]$$

where C is a constant lying between 0.001 and 0.003. Thus

$$r \propto \{1 + [288 - t(1 + \tfrac{1}{2}(\gamma - 1)M^2)]C\},$$

$$\frac{1}{r}\frac{\partial r}{\partial t} = -\frac{[1 + \tfrac{1}{2}(\gamma - 1)M^2]C}{1 + \{288 - t[1 + \tfrac{1}{2}(\gamma - 1)M^2]\}C}.$$

Substituting in equation (*a*) and neglecting $1/c$ compared with r,

$$\Pi_t = -(1+F/P)\left[\frac{C}{1+(288-T_1)C} + \frac{1}{T_1+z}\right]T_1,$$

where T_1 is, as noted already, a function of t and M. This equation applies at constant throttle opening: at constant boost pressure, the first term in the square brackets disappears.

To evaluate Π_r the procedure is as follows.

At constant pressure,

$$(V_1/P)\partial P/\partial V_1 = (M/P)\partial P/\partial M$$

$$= (1+F/P)\left[\frac{M}{r - 1/[c(1+\frac{1}{2}\eta_i\gamma M^2)]}\frac{\partial r}{\partial M} + \frac{\eta_i\gamma M^2}{1+\frac{1}{2}\eta_i\gamma M^2} - \frac{(\gamma-1)M^2 t}{T_1+z}\right].$$

Therefore

$$\Pi_r \approx (1+F/P)\left\{-(\gamma-1)M^2 t\left[\frac{C}{1+C(288-T_1)} + \frac{1}{T_1+z}\right] + \frac{\eta_i\gamma M^2}{1+\frac{1}{2}\eta_i\gamma M^2}\right\}$$

at constant throttle opening. At constant boost the formula reduces to

$$\Pi_r = -(1+F/P)(\gamma-1)M^2 t/(T_1+z).$$

REFERENCES

1. CAMERON, D. (1942). British Performance Reduction Methods for Modern Aircraft. A. & A.E.E. Report No. Res/170, 1942 (unpublished).
2. ANNAND, W. J. D. (1945). The Effects of the Use of Exhaust Thrust on Performance Reduction Methods. A. & A.E.E. Report No. Res/221, May 1945 (unpublished).
3. S.B.A.C. Standard Method of Propeller Performance Estimation (undated).
4. GARDINER and MULLIN (1949). The Design of Propellers. *Journal of the R.Ae.S.*, Vol. 53, p. 745, August 1949.

AXIALLY-SYMMETRICAL SUPERSONIC FLOW NEAR THE CENTRE OF AN EXPANSION

by

N. H. JOHANNESEN

(Mechanical Engineering Laboratory, The Technical University of Denmark)

and

R. E. MEYER

(Department of Mathematics, The University of Manchester)

SUMMARY

When a uniform, two-dimensional supersonic flow expands suddenly round a corner in a wall it forms a pattern known as a Prandtl-Meyer expansion or centred simple wave. If the flow is two-dimensional but not initially uniform, or if it is axially-symmetrical, the expansion is still centred, but is not a simple wave. An approximate solution is given in this paper for the isentropic, irrotational, steady two-dimensional or axially-symmetrical flow of a perfect gas in the neighbourhood of the centre of such an expansion. The solution is designed to replace the conventional method of characteristics in such a region.

The main application is to a jet issuing from a nozzle that discharges into a container with a pressure lower than that in the nozzle; in particular, a formula is derived for the initial curvature, at the lip of the nozzle, of the boundary of the jet. The solution also applies to the flow near an edge in a boundary wall, and a formula is derived for the velocity gradient on the wall immediately downstream of the edge.

1. INTRODUCTION

The present investigation was stimulated by the research on steam- and air-jet ejectors carried out by one of the authors, who was able to show that several experimental results concerning ejectors may be explained theoretically if certain aerodynamic features of the actuating jet can be calculated[1]. The experimental evidence indicates a correlation between the behaviour of an ejector, with given shape of the ducts, and the position of, and the flow conditions at, the point P where the boundary of the actuating jet (or rather the mixing zone that develops along it) meets the wall of the diffuser (Fig. 1).

A similar physical problem occurs with a thrust augmenter for aircraft propulsion if one of the two mixing gas streams is supersonic.

Paper received March 1949.

[The Aeronautical Quarterly, Vol. II, August 1950]

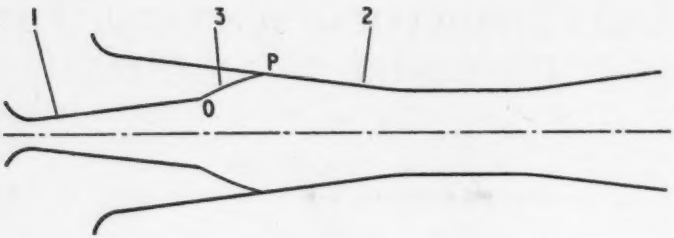

Fig. 1.

(1) Actuating nozzle, (2) Diffuser, (3) Jet boundary, *0* Lip of nozzle.

In order to compute the boundary of the actuating jet by the method of characteristics it was found desirable to obtain an approximate solution for the field of flow near the lip of an axially-symmetrical, supersonic nozzle. Such a solution was therefore sought (Section 2) in the form of an expansion in powers of the ratio, R, of the distance from the lip to the distance of the lip from the axis (Fig. 2).

The field of flow in the neighbourhood of the lip of a nozzle may be divided into three parts, namely the centred expansion and the regions upstream and downstream of it. The first term in a series expansion with respect to R is identical with the solution of the corresponding two-dimensional flow problem; to this approximation, the flow is uniform in the regions upstream and downstream of the expansion, and of the Prandtl-Meyer type in the region of the expansion[2]. The equations for the second term in the expansion are integrated for axially symmetrical flow in Sections 3 and 4. From the resulting formulæ the velocity components can be calculated (with an error of the order of R^2) and the initial curvatures of the jet boundary and of the Mach lines in the expansion region can be determined (Section 6).

The solution applies also to the flow in the neighbourhood of an edge in the surface of a body of revolution, or in the wall of a duct of circular cross-section. In such cases the velocity gradient on the wall just downstream of the edge may be determined (Section 6).

The corresponding formulæ for two-dimensional flow are given in Section 8 (equations (33) to (35)).

In a jet issuing from an axially-symmetrical nozzle a limit line, and hence a shockwave, may be encountered that starts on the downstream border of the region of centred expansion. Knowledge of the initial curvature of the jet boundary permits an estimate to be obtained for the position at which the shockwave starts (Section 7 and Appendix).

AXIALLY-SYMMETRICAL SUPERSONIC FLOW

The calculations are carried through for the case of a perfect gas without viscosity or heat conductivity, and the flow is assumed to be isentropic, irrotational, steady, and shock-free. The results, therefore, apply only to the case where an expansion does in fact take place at the lip of the nozzle or the edge on the surface. By introducing the shockwave equations instead of the solution for a centred expansion, the method could be adapted to an approximate treatment of the flow in the neighbourhood of a lip, or edge, with an attached shockwave.

Notation

r	distance from the axis of symmetry
R	ratio of the distance from the centre of the expansion to the distance of the centre from the axis
R, ϕ	polar co-ordinates in the meridian plane with origin at the centre of the expansion (Fig. 2)
u, v	velocity components in the directions of R and ϕ increasing, respectively (Fig. 2)
q	velocity magnitude
θ	angle between the downstream direction on the axis and the local stream direction
a	local speed of sound
a_*	critical speed of sound
μ	local Mach angle ($\sin \mu = a/q$)
u_0, v_0, a_0	first terms in the expansions of u, v, a, respectively, in powers of R (values at the centre of the expansion)
u_1, v_1, a_1	coefficients of R in the expansions of u, v, a, respectively, in powers of R
q_0, w	velocity magnitude at the centre of the expansion in regions of type A and B, respectively
M	Mach number at centre of expansion ($M = q_0/a_0$)
$I_1(\eta) \ldots I_4(\eta)$	integrals occurring in equation (14)
$P(\mu)$	Busemann's "Pressure number"
h_β	focusing parameter of Ref. 4
$A_1, C_1, C_2, K_1, \beta_0, \beta_1, \beta_2$	constants of integration

S $2(a_0^2/w)\cos\beta_1$

y rectangular co-ordinate

γ adiabatic exponent

δ angle of deflection of the streamline at the centre of the expansion

Δ angle at the centre containing the region of centred expansion

λ $[(\gamma-1)/(\gamma+1)]^{\frac{1}{2}}$

η $\lambda(\phi+\beta_0)$

ψ $\phi-\beta_1$

Suffixes:

$_B$ limiting value as the centre of the expansion is approached along the boundary streamline

$_c$ limiting value as the centre is approached along the boundary streamline from upstream

$_J$ limiting value as the centre is approached along the boundary streamline from downstream

$_L$ limiting value as the centre is approached along the leading Mach line of the region of centred expansion

$_F$ limiting value as the centre is approached along the final Mach line of the region of centred expansion

2. EQUATIONS OF MOTION

Let the radius of the nozzle mouth be taken as the unit of length. We introduce a system of polar co-ordinates R, ϕ in a meridian plane, with origin at the lip and with ϕ measured in the counter-clockwise sense from the normal to the axis through the lip (Fig. 2). All the dependent variables are assumed expanded in powers of R, with coefficients depending on ϕ. Thus, if u and v denote the velocity components in the directions of R and ϕ increasing, respectively,

$$\left.\begin{aligned} u(R,\ \phi) &= u_0(\phi)+Ru_1(\phi)+R^2u_2(\phi)+\ldots \\ v(R,\phi) &= v_0(\phi)+Rv_1(\phi)+\ldots \end{aligned}\right\} \quad . \quad . \quad . \quad (1)$$

The absence of vorticity is expressed by the equation

$$\frac{\partial u}{R\partial\phi}-\frac{1}{R}\frac{\partial(Rv)}{\partial R}=0 \quad . \quad . \quad . \quad . \quad . \quad (2)$$

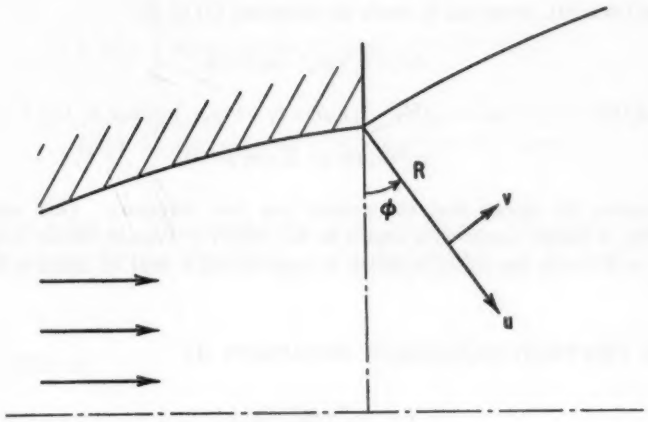

Fig. 2.

The equations of continuity and of motion may be combined to give the equation*

$$(u^2-a^2)\frac{\partial u}{\partial R}+(v^2-a^2)\frac{\partial v}{R\partial\phi}+uv\left(\frac{\partial v}{\partial R}+\frac{\partial u}{R\partial\phi}\right)-a^2\frac{u}{R}-\frac{a^2}{1-R\cos\phi}(v\sin\phi-u\cos\phi)=0. \quad . \quad . \quad . \quad . \quad . \quad . \quad . \quad . \quad (3)$$

Bernoulli's equation is

$$u^2+v^2+\frac{2}{\gamma-1}a^2=\lambda^{-2}a_*^2, \quad . \quad . \quad . \quad . \quad . \quad . \quad (4)$$

where a is the local speed of sound, a_* the critical speed of sound, and $\lambda^2=(\gamma-1)/(\gamma+1)$.

If the series (1) be substituted into (2) and coefficients of the various powers of R are equated the following are obtained:

$$v_0=u_0', \quad . \quad . \quad . \quad . \quad . \quad . \quad . \quad . \quad (5)$$

$$v_1=\tfrac{1}{2}u_1', \quad . \quad . \quad . \quad . \quad . \quad . \quad . \quad (6)$$

etc., where dashes denote differentiation with respect to ϕ. Similarly, from (4),

$$u_0^2+v_0^2+\frac{2}{\gamma-1}a_0^2=\lambda^{-2}a_*^2, \quad . \quad . \quad . \quad . \quad . \quad (7)$$

$$u_0u_1+v_0v_1+\frac{2}{\gamma-1}a_0a_1=0, \quad . \quad . \quad . \quad . \quad . \quad . \quad (8)$$

* It can be obtained, for example, from the equations (7*), (8) and (10) for motion in general orthogonal co-ordinates in a meridian plane in Ref. 3.

and then from (3), when use is made of equations (5) to (8),

$$(u_0+v_0')(v_0^2-a_0^2)=0, \quad . \quad . \quad . \quad . \quad . \quad (9)$$

$$(v_0^2-a_0^2)(v_1'+u_1)+(u_0+v_0')[(\gamma-1)u_0u_1+(\gamma+1)v_0v_1]+2u_0v_0v_1+(u_0^2-a_0^2)u_1-$$
$$-a_0^2(v_0\sin\phi-u_0\cos\phi)=0. \quad . \quad . \quad . \quad . \quad (10)$$

Equation (9) shows that the system has two solutions. One, solution *A*, approaches a simple wave with centre at the origin ("Prandtl-Meyer Expansion," Ref. 2), as $R\longrightarrow 0$; the other, solution *B*, approaches a field of uniform flow.

3. THE CENTRED EXPANSION (SOLUTION *A*)

If

$$v_0^2-a_0^2=0 \quad . \quad . \quad . \quad . \quad . \quad . \quad (11)$$

(5) and (7) integrate to

$$\left.\begin{aligned} u_0(\phi)&=(a_*/\lambda)\sin[\lambda(\phi+\beta_0)],\\ v_0(\phi)&=a_*\cos[\lambda(\phi+\beta_0)],\\ q_0^2=u_0^2+v_0^2&=a_*^2\left(1+\frac{2}{\gamma-1}\sin^2[\lambda(\phi+\beta_0)]\right)\end{aligned}\right\} \quad . \quad . \quad . \quad (12)$$

(Ref. 2), where β_0 is a constant. By (11), equation (10) reduces to

$$2u_0u_1'+\left[\frac{3\gamma-1}{\gamma+1}(u_0/v_0)^2-1\right]v_0u_1-v_0(v_0\sin\phi-u_0\cos\phi)=0, \quad . \quad (13)$$

and after substituting from (12) this integrates to

$$u_1(\phi)=-\frac{a_*}{2\lambda}(\cos\eta)^{\frac{1}{2}(3\gamma-1)/(\gamma-1)}(\sin\eta)^{\frac{1}{2}}\times$$
$$\times\{I_1(\eta)\cos\beta_0+I_2(\eta)\sin\beta_0-\lambda I_3(\eta)\cos\beta_0+\lambda I_4(\eta)\sin\beta_0+C_1\}, \quad (14)$$

where $\eta=\lambda(\phi+\beta_0)$, C_1 is an arbitrary constant, and

$$I_1(\eta)=\int_{\eta_L}^{\eta}\cos(y/\lambda)(\sin y)^{-\frac{1}{2}}(\cos y)^{-1/(2\lambda^2)}\,dy,$$

$$I_2(\eta)=\int_{\eta_L}^{\eta}\sin(y/\lambda)(\sin y)^{-\frac{1}{2}}(\cos y)^{-1/(2\lambda^2)}\,dy,$$

$$I_3(\eta)=\int_{\eta_L}^{\eta}\sin(y/\lambda)(\sin y)^{-\frac{3}{2}}(\cos y)^{\frac{1}{2}(\gamma-3)/(\gamma-1)}\,dy,$$

$$I_4(\eta)=\int_{\eta_L}^{\eta}\cos(y/\lambda)(\sin y)^{-\frac{3}{2}}(\cos y)^{\frac{1}{2}(\gamma-3)/(\gamma-1)}\,dy,$$

(*cf.* Section 6, Table I). The introduction of the constant C_1 allows any convenient value to be chosen for the lower limit, η_L, in the integrals. v_1 is found from (6) and (13).

4. SOLUTION *B*

If

$$u_0+v_0'=0, \qquad (15)$$

it follows from (5) that

$$\left.\begin{aligned}u_0&=w\cos\psi,\\ v_0&=-w\sin\psi,\end{aligned}\right\} \qquad (16)$$

with

$$\left.\begin{aligned}w^2&=u_0^2+v_0^2=\text{constant},\\ \phi-\psi&=\text{constant}=\beta_1.\end{aligned}\right\} \qquad (17)$$

By (15), (6), and (17), equation (10) reduces to

$$\tfrac{1}{2}(v_0^2-a_0^2)u_1''+u_0v_0u_1'+(w^2-2a_0^2)u_1-a_0^2(v_0\sin\phi-u_0\cos\phi)=0, \qquad (18)$$

and upon substituting (16) we obtain the equation

$$(\sin^2\psi-a_0^2/w^2)u_1''-2\sin\psi\cos\psi\,u_1'+2(1-2a_0^2/w^2)u_1+S=0, \qquad (19)$$

where $S=2(a_0^2/w)\cos\beta_1$. The general solution of (19) is

$$u_1(\phi)=A_1\cos(2\psi+\beta_2)+K_1, \qquad (20)$$

provided the constants A_1, K_1, β_2 satisfy the relation

$$A_1\cos\beta_2+K_1(1-2a_0^2/w^2)+\tfrac{1}{2}S=0, \qquad (21)$$

as can be verified by substituting into (19). By (6),

$$v_1(\phi)=-A_1\sin(2\psi+\beta_2). \qquad (22)$$

5. BOUNDARY CONDITIONS

It will be convenient for the application of these results in the following sections to consider as separate branches the upstream and downstream parts of the streamline through the origin. On either of them ϕ and θ (the angle that the stream direction makes with the axis) may be regarded as functions of R, and near the origin,

$$\left.\begin{aligned}\phi &= \phi_B + (d\phi/dR)\,R + O(R^2),\\ \theta &= \theta_B + [(\partial\theta/\partial\phi)(d\phi/dR) + \partial\theta/\partial R]\,R + O(R^2),\end{aligned}\right\} \quad . \quad . \quad (23)$$

where the derivatives are taken for $\phi=\phi_B$, $R=0$. From Fig. 2,

$$\theta = \phi - \tfrac{1}{2}\pi + \tan^{-1}(v/u), \quad . \quad . \quad . \quad . \quad . \quad (24)$$

and if the streamline belongs to a region where the solution is of the type B, $\partial\theta/\partial\phi=0$ by (16) and (17); moreover, $v(0,\phi_B)=v_0(\phi_B)=0$, so that the curvature of the streamline at the origin becomes

$$(d\theta/dR)_{R=0} = v_1(\phi_B)/u_0(\phi_B) \quad . \quad . \quad . \quad . \quad (25)$$

(except for the sign in the case of the upstream branch).

Similarly,

$$q\,dq/dR = q(\partial q/\partial\phi)(d\phi/dR) + q\,\partial q/\partial R$$

on either branch of the streamline; if it belongs to a B region, $\partial q/\partial\phi=0$, and

$$q\,dq/dR = u_0(\phi_B)\,u_1(\phi_B) + O(R). \quad . \quad . \quad . \quad . \quad (26)$$

It may be noted that v_1 must be a discontinuous function of ϕ on the border between an A region and a B region, by (6), (13) and (18). The Mach line that separates the two regions must carry a first order disturbance[4]. However, the total derivatives of q and θ along the Mach line must be continuous, and it follows from the continuity of either that the limiting value of v_1 in the B region must exceed that in the A region by $(q\cos\mu)/(\gamma+1)$ times the initial curvature of the border Mach line, where q and μ are taken at the origin in the B region.

6. INITIAL CURVATURE OF A JET BOUNDARY

The centre of the expansion is at the lip of the nozzle. Let ϕ_C, ϕ_L, ϕ_F, and ϕ_J denote the limiting values of ϕ as $R \longrightarrow 0$ on the nozzle wall, on the leading and

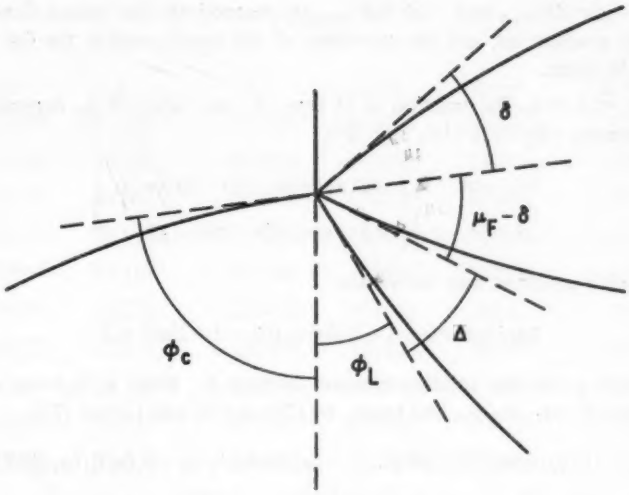

Fig. 3.

final Mach lines of the expansion region, and on the jet boundary, respectively (Fig. 3). Then

$$\left.\begin{aligned} \phi_L &= \pi - \mu_L + \phi_c, \\ \phi_F - \phi_L &= \Delta, \\ \phi_J - \phi_F &= \mu_F, \\ \Delta + \mu_F &= \delta + \mu_L, \end{aligned}\right\} \quad . \quad . \quad . \quad . \quad . \quad (27)$$

where μ_L and μ_F are the Mach angles corresponding to the ultimate speed, q_L, on the nozzle wall and to the speed, q_F, on the free boundary of the jet, respectively. Δ is the angle at the lip containing the expansion region, δ the angle of deflection of the boundary streamline.

For $\phi_c \leqslant \phi \leqslant \phi_L$ the solution is of type B; it is not influenced by the fact that the nozzle ends at the origin. Since $u_0(\phi_c) = -q_L$, $v_0(\phi_c) = 0$, we may put $w = q_L$, $\psi = \phi - \phi_c$, in this region, whence

$$u_0(\phi_L) = q_L \cos \mu_L, \quad v_0(\phi_L) = q_L \sin \mu_L, \quad . \quad . \quad . \quad (28)$$

by (16), (17), and (27). By (20) to (22) and (25) to (27),

$$\begin{aligned} u_1(\phi_L) &= 2\cos^2 \mu_L \, u_1(\phi_c) - \sin 2\mu_L \, v_1(\phi_c) + \tfrac{1}{2}S \\ &= q_L \sin 2\mu_L \left[(d\theta/dR)_{R=0} - (1/q_L)\cot \mu_L (dq/dR)_{R=0}\right] - q_L \sin \theta_c \sin^2 \mu_L, \end{aligned} \quad (29)$$

where θ_c, $-(dq/dR)_{R=0}$, and $-(d\theta/dR)_{R=0}$ are respectively the stream direction and the velocity gradient on, and the curvature of, the nozzle wall at the lip; these we assume to be given.

For $\phi_L \leqslant \phi \leqslant \phi_F$ the solution is of type *A*; the value of ϕ_F depends on the outside pressure. By (12), (16), and (27),

$$\left.\begin{aligned} \lambda\Delta &= \cot^{-1}(\lambda^{-1}\tan\mu_F) - \cot^{-1}(\lambda^{-1}\tan\mu_L), \\ \beta_0 &= \mu_L - \pi - \phi_c + \lambda^{-1}\cot^{-1}(\lambda^{-1}\tan\mu_L),* \end{aligned}\right\} \quad . \quad . \quad . \quad (30)$$

and Bernoulli's equation may be written

$$(q_F/q_L)^2 = (\gamma - 1 + 2\sin^2\mu_L)/(\gamma - 1 + 2\sin^2\mu_F). \quad . \quad . \quad . \quad (31)$$

For $\phi_F \leqslant \phi \leqslant \phi_J$ the solution is again of type *B*. Since $u_0(\phi_J) = q_F$, $v_0(\phi_J) = 0$ we have now $\beta_1 = \phi_J$, $w = q_F$, and hence, by (20) to (22) and (25) to (27),

$$(d\theta/dR)_{R=0} - (1/q_F)\cot\mu_F (dq/dR)_{R=0} = -[q_F \sin\theta_J \sin^2\mu_F + u_1(\phi_F)]/(q_F \sin 2\mu_F) \quad (32)$$

on the downstream branch of the boundary streamline; $\theta_J = \phi_J - \frac{1}{2}\pi$ is the stream direction just downstream of the centre of the expansion. In the case of a jet, $dq/dR = 0$ on its boundary, and (32) gives the initial curvature of the jet boundary. If the centred expansion arises from an edge on the wall of an axially-symmetrical duct, $d\theta/dR$ is given on the wall, and from (32) we may calculate the velocity gradient on the wall just downstream of the edge.

For the calculation of the initial slope and curvature of the jet boundary, the following steps are necessary. First, μ_L and $u_1(\phi_L)$ must be calculated from the known conditions on the nozzle wall, immediately upstream of the lip (equation (29)). Secondly, q_F must be found from the known pressure outside the jet and the initial

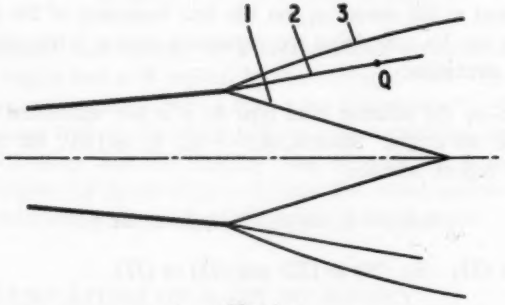

Fig. 4.
(1) Leading Mach line, (2) Final Mach line, (3) Jet boundary.

* A table of $P(\mu) = 1{,}090° - \mu - (180°/\pi)\,\lambda^{-1}\cot^{-1}(\lambda^{-1}\tan\mu)$ is given in Ref. 5.

TABLE I

$\sin\eta$	η	$I_1(\eta)$	$I_2(\eta)$	$I_3(\eta)$	$I_4(\eta)$
.73167	47°.026	−.025191	.056596	.053642	−.023868
.74348	48.029	−.054656	.115879	.107910	−.050833
.75530	49.052	−.089006	.178076	.162857	−.081169
.76712	50.096	−.128971	.243441	.218536	−.115202
.77894	51.163	−.175440	.312256	.274999	−.153318
.79076	52.256	−.229498	.384842	.332301	−.195981
.80257	53.377	−.292490	.461560	.390495	−.243748
.81439	54.527	−.366095	.542815	.449630	−.297298
.82621	55.711	−.452442	.629062	.509751	−.357467
.83803	56.933	−.554272	.720812	.570885	−.425293

for $\sin\eta_L=.71985$ ($\eta_L=46°.0420$) and $\gamma=7/5$ (for air).

state of the gas. μ_F and Δ can then be calculated from (31) and (30), and δ follows from (27).* $u_1(\phi_F)$ is found from (14), where the integrals have to be evaluated between the limits $\eta_L=\cot^{-1}(\lambda^{-1}\tan\mu_L)$ and $\eta=\eta_L+\lambda\Delta$. Finally, the initial curvature of the jet boundary is given by (32), with $(dq/dR)_{R=0}=0$.

The integrals that occur in (14) have been tabulated in Ref. 1 for $46°.0420\leqslant\eta\leqslant56°.9326$—these values correspond, for air with $\gamma=7/5$, to the Mach numbers 2.7300 and 3.8928—and the table is reproduced in Table I; it covers all cases of expansions with initial and final Mach numbers between those limits.

7. THE POSITION OF THE POINT AT WHICH THE SHOCKWAVE STARTS

In Ref. 1 the computation of the field of flow has been carried further in a particular case by the method of characteristics. The nozzle was taken to generate a pure source flow in a cone of semi-vertex angle 4°, with a Mach number 2.7300 at the lip (so that $\phi_0=-86°$ and $\phi_L=72°.51$; Fig. 4). A centred expansion to $M=3.893$ is then found to lead to a deflection of the boundary streamline through $\delta=20°.074$ ($\Delta=26°.68$ and $\phi_F=99°.19$; it was also found that $u_1(\phi_L)/u_0(\phi_L)=0.0302$ and $u_1(\phi_F)/u_0(\phi_F)=0.0226$). No use was made of

* In the case of an edge in the wall, δ is given and μ_F is found by the help of the $P,\mu-$table, for $P(\mu_L)-P(\mu_F)=\mu_F-\mu_L+\Delta=\delta$ by (27) and (30)[2].

equation (32) in computing the boundary of the jet; this equation predicts an initial radius of curvature $|dR/d\theta| = 10.175$, a value which is found to agree well with the results of the computation of Ref. 1.

It is of interest to examine how far the results of the present investigation, together with those of earlier publications, permit an estimation of the position at which the first shockwave will start in a jet of this type. The considerations will be based on the well-known conjecture[6] that the shockwave starts either where a limit line starts, or at the cusp of a limit line. It is to be expected that the region of the centred expansion will not contain a limit line. If the downstream border of this region, *i.e.* the final Mach line, meets a limit line the position of its limit point can be determined by a method indicated in Ref. 4, where a length parameter h_β is introduced that vanishes at the limit point and a differential equation is given that governs the variation of h_β on a Mach line (equation (43) of Ref. 4). To integrate this "focusing" equation it is necessary to know (*i*) the initial value of h_β on the downstream side of the final Mach line, at the centre of the expansion, and (*ii*) the velocity distribution on this Mach line, on which the coefficients of the equation depend. The former is given exactly by the present theory, but the velocity distribution remains unknown except for the values of the velocity components and their derivatives at the lip. In the absence of further information estimates can only be substituted for the coefficients in the focusing equation of Ref. 4, based on their known values at the lip.

In this way, two estimates are derived in the Appendix for the position of the point where the shockwave starts. For the special case of Ref. 1, equation (A1) predicts a limit line starting where $r = 1.35$ on the final Mach line (r denotes the distance from the axis). The more refined estimate (A4) gives $r = 1.315$. In Ref. 1 the first intersection of adjacent Mach lines of the characteristic network is found to occur at Q (Fig. 4), where $r = 1.426$ on the final Mach line of the expansion region. This result, however, depends on the step size employed for the numerical process, and from it it may be concluded only that the limit line starts on this Mach line somewhere between the points where $r = 1$* and $r = 1.426$.

8. COMPARISON WITH THE TWO-DIMENSIONAL CASE

For the two-dimensional flow near the centre of an expansion the equations (1) to (13), and (15) to (28), remain valid if the last term on the left hand side is deleted in equations (3), (10), (13), (18), (19), and (21). Hence, the solution B in the two-dimensional case is obtained from that in Section 4 by putting S equal to zero, and

* The limit line cannot start at the lip itself. For if the lip were a point of an envelope of the Mach lines of the region downstream of the centred expansion, the initial curvature of the jet boundary would be infinite, and this is not the case.

instead of equations (29) and (32) we have

$$u_1(\phi_L)=q_L \sin 2\mu_L [(d\theta/dR)_{R=0}-(1/q_L)\ \cot\mu_L (dq/dR)_{R=0}], \quad . \quad . \quad (33)$$

and $$(d\theta/dR)_{R=0}-(1/q_T)\cot\mu_T (dq/dR)_{R=0}=-u_1(\phi_T)/(q_T \sin 2\mu_T), \quad . \quad (34)$$

respectively. For solution A we now find

$$u_1(\phi)=C_2 [\sin\eta (\cos\eta)^{(3\gamma-1)/(\gamma-1)}]^{\frac{1}{2}}, \quad . \quad . \quad . \quad (35)$$

instead of (14), where C_2 is a constant of integration. In two-dimensional flow the expression

$$\beta=\theta-\int (1/q)\cot\mu\ dq$$

is a characteristic parameter[6], and equations (33) to (35) show that its derivative in the stream direction increases from the upstream side to the downstream side of the centre of an expansion in the same ratio as the expression

$$[\sin\eta (\cos\eta)^{(3\gamma-1)/(\gamma-1)}]^{\frac{1}{2}}/(q \sin 2\mu),$$

where $\eta=\cot^{-1}(\lambda^{-1}\tan\mu)$.*

The equations (32) and (34) differ by a term which is proportional to the radial velocity component just downstream of the lip; if this component of the velocity is positive the additional term reduces the initial curvature of the jet boundary, and hence encourages the formation of a shockwave in the case of axially-symmetrical flow (*cf.* Appendix). On the other hand, a low value of $u_1(\phi_T)$ is seen to discourage the breakdown of potential flow. Equation (13) shows that an increase (decrease) in the magnitude of u_1 in the transition through the centred expansion is common to two-dimensional and axially-symmetrical flow if $M<(>)\sqrt{\{4\gamma/(3\gamma-1)\}}$; if the radial velocity is positive, the last term in (13) favours an increase in u_1, and thus hastens the formation of a shock. A positive radial velocity at the lip just upstream of the expansion, however, is seen to reduce the initial value of u_1 in the expansion region (equation (29)).

ACKNOWLEDGMENTS

The authors wish to thank Professor S. Goldstein and Professor J. L. Mansa for their advice, and for their help in making the authors' co-operation possible.

* $2\cos\mu$ times this derivative of β is increased by the reciprocal of the growth factor which governs the steepening of wave fronts in two-dimensional flow [6].

APPENDIX

(The notation used is that of Ref. 4)

Estimates for the position of the point where the shockwave starts

Additional symbols not included in the main notation given on pages 129 *and* 130

ϵ	$\theta-\mu$
R_{s_1}	radius of curvature of the free boundary at the lip
τ	$\log r$
ν^2	e^2-g
n^2	$g-e^2$
κ_β	curvature of Mach line

If the curvature of the final Mach line of the expansion region and the variation of the velocity components along it are neglected, *i.e.* if equations (44) of Ref. 4 are assumed to hold, equation (51) of Ref. 4 remains valid; the streamline curvature at the lip, as defined in Ref. 4, is $-(d\theta/dR)_{R=0}$. If, in addition, the radial velocity component on the final Mach line is neglected, so that (44*a*) holds, but it is not assumed that this Mach line is inclined to the axis at the Mach angle, then equation (52) of Ref. 4 remains valid, provided N is replaced by

$$N' = -(\gamma+1)/\{\cos^2\mu \sin\mu \sin(\theta-\mu)\},$$

where $\theta-\mu=\epsilon$ is the inclination of the final Mach line. Thus h_β vanishes, and the shockwave may be assumed to start, where

$$r^4 = 1+\frac{1}{\gamma+1} R_{s_1} \cos^2\mu \sin\mu \sin(\theta-\mu) \quad . \quad . \quad . \quad \text{(A1)}$$

on the final Mach line, with

$$R_{s_1} = -(dR/d\theta)_{R=0}.$$

If it is assumed that equations (44) but not (44*a*) of Ref. 4 hold on the final Mach line, *i.e.* that the radial velocity component is constant on it and equal to its value at the lip*, equation (83) of Ref. 4† reduces to‡

$$\frac{d^2h_\beta}{dr^2} + \frac{2e+1}{r}\frac{dh_\beta}{dr} + \frac{g}{r^2}h_\beta = 0, \quad . \quad . \quad . \quad . \quad \text{(A2)}$$

---

* It should be noted that neither approximation is consistent in the sense that a characteristic with the properties assumed could exist. For it is shown [7] that if a Mach line in isentropic, irrotational, axially-symmetrical, steady, supersonic flow is straight and if the velocity components are constant along it, then the radial velocity component must vanish on it, and its inclination to the axis must be equal to the Mach angle.

† In that equation, the first term in the square bracket should read $2v_\beta R/v_a^2$; and the left hand side of equation (84) should read $\partial R/h_\beta \partial\beta$. The definition of λ given in Ref. 4 differs from the one adopted here.

‡ Since a single Mach line is being considered, it can be assumed without loss of generality that $\partial h_\alpha/\partial\alpha = 0$.

with $e = -\dfrac{\sin\theta}{8\cos\mu\sin\epsilon}\left[\dfrac{2}{\sin\theta}(\cos\mu\sin\epsilon+\sin(\mu+\epsilon))+(\gamma+1)(\tan^2\mu-1)\right]$,

$$g=\frac{\sin^2\theta}{4\cos^2\mu\sin^2\epsilon}\left(2(\gamma-1)+\frac{\sin\mu}{\sin\theta}\left[(\gamma+1)\frac{\cos\theta}{\cos\mu}+(\gamma-1)\cos\epsilon\right]\right).$$

(A2) can be written

$$d^2y/d\tau^2+(g-e^2)\,y=0,$$

with $y=r^e h_\beta$ and $\tau=\log r$. If $\nu^2=e^2-g>0$*, h_β vanishes for

$$r^{2\nu}=\left(\frac{dy/dr-\nu y}{dy/dr+\nu y}\right)_{r=1}. \qquad \text{(A3)}$$

If $n^2=g-e^2>0$†, h_β vanishes for

$$n\log r=-\tan^{-1}\left(\frac{ny}{r\,dy/dr}\right)_{r=1}. \qquad \text{(A4)}$$

Now

$$\frac{dy}{dr}=y\left(\frac{e}{r}+\frac{1}{h_\beta}\frac{dh_\beta}{dr}\right)=y\left(\frac{e}{r}+\frac{\kappa_\beta}{\sin\epsilon}\right),$$

by (3) of Ref. 3, and it may be assumed without loss of generality that $h_\beta=1$ (and hence $y=1$) for $r=1$ on the Mach line. Since it is a "plus Mach line," the upper sign must be taken in equation (51) of Ref. 4 and $\epsilon=\theta-\mu$, whence

$$(dy/dr)_{r=1}=e-(\gamma+1)/\{2\cos^2\mu\sin\mu\sin(\theta-\mu)\,R_{S_1}\}$$

where $$1/R_{S_1}=-(d\theta/dR)_{R=0}$$

in the notation employed in Sections 5-7 above.

---

* In the case treated in Ref. 4, $g=0$ and $e=-1/4$.

† This sign is found to hold in the case discussed in Section 7 above.

REFERENCES

1. JOHANNESEN, N. H., *Ejector Theory and Experiments*, Copenhagen (in the press).

2. TAYLOR, G. I., and MACCOLL, J. W. (1935). *Aerodynamic Theory* (edited by Durand), Berlin, Vol. III, Div. H., Chap. IV, pp. 243-246, 1935.

3. MEYER, R. E. (1948). The Method of Characteristics for Problems of Compressible Flow Involving Two Independent Variables. Part I. *Quarterly Journal of Mechanics and Applied Mathematics*, Vol. 1, pp. 196-219, 1948.

4. MEYER, R. E. (1948). The Method of Characteristics for Problems of Compressible Flow Involving Two Independent Variables. Part II. *Quarterly Journal of Mechanics and Applied Mathematics*, Vol. 1, pp. 451-469, 1948.

5. HERBERT, P. J., and OLDER, S. J. (1946). Tables for Use in the Investigation of Supersonic Fields of Flow by the Method of Characteristics. A.R.C. 10261, 1946.

6. MEYER, R. E. (1949). Focusing Effects in Two-Dimensional, Supersonic Flow. *Philosophical Transactions of the Royal Society*, London, *A*, Vol. 242, pp. 153-171, 1949.

7. HOLT, M. (1948). The Behaviour of the Velocity along a Straight Characteristic in Steady Irrotational Isentropic Flow with Axial Symmetry. *Quarterly Journal of Mechanics and Applied Mathematics*. Vol. 1, pp. 358-364, 1948.

NOTE ON THE DEPENDENCE OF FLAP HINGE MOMENT DERIVATIVES ON HINGE POSITION

by

W. J. DUNCAN, D.Sc., F.R.S., F.R.Ae.S.

(Professor of Aerodynamics, College of Aeronautics, Cranfield)

SUMMARY

It is shown to be a consequence of kinematics and statics that the aerodynamic derivative expressing the rate of change of hinge moment of a plain flap with the angular setting of the flap varies parabolically with the chordwise position of the hinge. The derivative expressing the rate of change of hinge moment with incidence of the main surface varies linearly with the hinge position. Similar conclusions hold for the derivatives of the hinge moment with respect to the corresponding angular velocities.

The object of this note is to obtain all the information on hinge moment derivatives which can be obtained from kinematics and statics alone.

Take the main surface and flap in a certain datum configuration, placed in a uniform airstream of fixed characteristics and let the hinge be at a datum position in the chord line. For a given incidence of the main surface the aerodynamic forces on the flap will be statically equivalent to a force N, normal to the chord and through the hinge axis, a tangential or chordwise force T and a hinge moment H. The force T is small and will at present be neglected but its influence on the hinge moment would not be negligible if the hinge axis had a large vertical offset from the chord line. N is taken positive downwards and H positive in the trailing edge down sense. In general, N and H will depend on the angular deflection ξ and on z, the normal downward displacement of the flap*, and we shall express them by means of derivatives as follows

$$N = N_0 + z\frac{\partial N}{\partial z} + \xi\frac{\partial N}{\partial \xi} \quad . \quad . \quad . \quad . \quad . \quad (1)$$

$$H = H_0 + z\frac{\partial H}{\partial z} + \xi\frac{\partial H}{\partial \xi} \quad . \quad . \quad . \quad . \quad . \quad . \quad (2)$$

Now, with the flap in its datum configuration, let us shift the hinge axis rearward along the flap chord through the distance l, and then let the flap be deflected through

---

*The reason for introducing this will become apparent later.

Paper received January 1950.

[The Aeronautical Quarterly, Vol. II, August 1950]

the angle ξ. When ξ is small this raises the original hinge by the amount $l\xi$, *i.e.* $z=-l\xi$. Hence N and H, still referred to the original hinge axis, are given by

$$N=N_0+\xi\left(\frac{\partial N}{\partial \xi}-l\frac{\partial N}{\partial z}\right) \quad . \quad . \quad . \quad . \quad . \quad (3)$$

$$H=H_0+\xi\left(\frac{\partial H}{\partial \xi}-l\frac{\partial H}{\partial z}\right). \quad . \quad . \quad . \quad . \quad . \quad (4)$$

By statics the normal force N' and hinge moment H' referred to the new hinge axis are given by

$$N'=N \quad . \quad . \quad . \quad . \quad . \quad . \quad . \quad . \quad (5)$$

$$H'=H-Nl. \quad . \quad . \quad . \quad . \quad . \quad . \quad . \quad . \quad (6)$$

Hence by (3) and (4)

$$\frac{\partial N'}{\partial \xi}=\frac{\partial N}{\partial \xi}-l\frac{\partial N}{\partial z} \quad . \quad . \quad . \quad . \quad . \quad . \quad . \quad (7)$$

$$\frac{\partial H'}{\partial \xi}=\frac{\partial H}{\partial \xi}-l\left(\frac{\partial H}{\partial z}+\frac{\partial N}{\partial \xi}\right)+l^2\frac{\partial N}{\partial z}. \quad . \quad . \quad (8)$$

Thus the hinge moment derivative varies parabolically with hinge position. This simple fact will be obscured when the conventional non-dimensional coefficient b_2 (the rate of change of hinge moment coefficient with ξ) is calculated, on account of the division by the area of the flap aft of the hinge, since this varies as the hinge is shifted.

Suppose next that λ is some parameter affecting N and H but not involving change of position of flap relative to main surface. Then we derive immediately from (5) and (6) that

$$\frac{\partial N'}{\partial \lambda}=\frac{\partial N}{\partial \lambda} \quad . \quad . \quad . \quad . \quad . \quad . \quad . \quad . \quad (9)$$

and

$$\frac{\partial H'}{\partial \lambda}=\frac{\partial H}{\partial \lambda}-l\frac{\partial N}{\partial \lambda}. \quad . \quad . \quad . \quad . \quad . \quad . \quad . \quad (10)$$

In particular, if we identify λ with the angle of incidence α we derive

$$\frac{\partial H'}{\partial \alpha}=\frac{\partial H}{\partial \alpha}-l\frac{\partial N}{\partial \alpha}. \quad . \quad . \quad . \quad . \quad . \quad . \quad (11)$$

Hence this derivative varies linearly with hinge position. Again this simple result is masked in the conventional non-dimensional coefficient b_1 (the rate of change of hinge moment coefficient with α). Similar arguments apply to the damping derivatives. Thus, corresponding to (8) we have

$$\frac{\partial H'}{\partial \dot{\xi}} = \frac{\partial H}{\partial \dot{\xi}} - l\left(\frac{\partial H}{\partial \dot{z}} + \frac{\partial N}{\partial \dot{\xi}}\right) + l^2 \frac{\partial V}{\partial \dot{z}}, \quad . \quad . \quad (12)$$

while (11) corresponds to

$$\frac{\partial H'}{\partial \dot{\alpha}} = \frac{\partial H}{\partial \dot{\alpha}} - l\frac{\partial N}{\partial \dot{\alpha}}. \quad . \quad . \quad . \quad . \quad . \quad . \quad (13)$$

All the results given apply to flaps in two and three dimensions.

The author is not aware that the foregoing simple arguments have been published previously in an explicit form. However, the nature of the dependence of the derivatives on the chordwise position of the hinge is implicit in the work of Küssner and Schwarz[1] and of W. P. Jones[2] on flutter derivatives.

It is suggested that it may be a convenient technique in wind tunnel work on hinge moments to measure H and N and their dependence on ξ and z for a single chordwise hinge position rather than to use a succession of chordwise hinge positions.

REFERENCES

1. Küssner, H. G. and Schwarz, L. (1940). The Oscillating Wing with Aerodynamically Balanced Aileron. *Luftfahrtforschung*, Vol. 17, 1940.

2. Jones, W. P. (1941). Aerodynamic Forces on an Oscillating Aerofoil-Aileron-Tab Combination. R. & M. 1948, 1941.

ON THE CHORDWISE LIFT DISTRIBUTION AT THE CENTRE OF SWEPT WINGS

by

D. KÜCHEMANN
and
J. WEBER
(Aerodynamics Department, Royal Aircraft Establishment)

SUMMARY

The present note deals with the peculiarities of the lift distribution on swept wings. The influence of the angle of sweep is expected to be greatest in its effect on the chordwise lift distribution at the centre section of the wing. It is assumed that the essential characteristics of this chordwise lift distribution are predominantly determined by the special configuration of the bound vortices and not so much by the trailing vortices. In calculating the downwash, induced by a continuous chordwise distribution of swept vortex lines of infinite span, it is found that the downwash at the centre line is to be expected to differ from its two-dimensional form mainly by a term proportional to the local vortex strength. Solutions of this simplified downwash equation have been obtained. They differ from the ordinary flat-plate distribution only in the exponent which instead of $\frac{1}{2}$ becomes $\frac{1}{2} - \phi/\pi$. It is suggested that this type of function is more appropriate for the centre-section of swept wings and that it may replace the ordinary flat-plate distribution in all those cases where the lifting surface is swept.

1. INTRODUCTION

It is known that both the spanwise and the chordwise lift distribution on swept wings show appreciable differences from those on straight wings. The chordwise lift distribution in the centre region in particular differs essentially from the distribution on two-dimensional aerofoils. Generally, the chordwise lift farther out on the wing resembles that on unswept two-dimensional wings and, for uncambered aerofoil sections, the "flat-plate" distribution is known to give a good first approximation. At the centre-section, of swept-back wings, however, the local lift in the front part of the section, as shown by experiments, is reduced compared with that of the flat plate; whereas the rear part shows a somewhat higher local lift. This generally results in a reduction of the local lift coefficient and also in a rearward displacement of the aerodynamic centre. These changes are greatest in the plane of symmetry. The flat-plate distribution cannot give a sufficiently accurate first approximation in this case and more terms of the Birnbaum-series for the chordwise lift distribution are needed if the ordinary method is to be applied. Attempts should be made therefore to find a function whose first

Paper received January 1950.
[The Aeronautical Quarterly, Vol. II, August 1950]

term would give a satisfactory first approximation. The present note suggests a type of distribution which might be appropriate and which may thus replace the flat-plate distribution in the plane of symmetry in all those cases where the lifting surface is swept.

In order to simplify the mathematical approach it is assumed that the essential characteristics of the chordwise lift distribution are predominantly determined by the special configuration of the bound vortices and not so much by the trailing vortices. The trailing vortices are neglected therefore; and a swept wing of infinite span with a constant spanwise lift distribution is taken as a basis.

To calculate the lift distribution at the centre of the wing the downwash field of a given vortex distribution is first needed. In determining the downwash, induced by a continuous distribution of swept vortex lines along the chord, it is found necessary to avoid the usual simplification of calculating the value on the chordline; the proper limit as z (the vertical co-ordinate) tends to zero has to be taken. Since one of the downwash terms tends to infinity at the chordline, a further simplification is suggested tentatively, allowing either for the finite thickness of the wing profile or for a suitable rounding off of the vortex lines at the centre. The downwash is assumed to differ from its two-dimensional form only by a term proportional to the local vortex strength. Solutions to the simplified downwash equation are then obtained (equation (13)). Values for one of the parameters in this solution are determined by using some experimental data. Finally, an expression for the chordwise lift distribution at the centre is obtained, where only a general factor, *i.e.* the total lift coefficient, remains to be determined. This must be left to a more complete investigation where the effect of the trailing vortices is included. But the type of distribution found agrees fairly well with experimental data and appears to cater for the effect of the angle of sweep.

Notation

x, y, z	rectangular co-ordinate system; x in direction of flight; y to starboard; z downwards
c	wing chord
h	distance of aerodynamic centre from leading edge
α	angle of incidence
ϕ	angle of sweep
V_0	velocity of main flow
v_x	velocity increment in x-direction
v_z	induced velocity in z-direction
Γ	strength of isolated vortex line
γ	vorticity of continuous vortex distribution
ΔC_p	difference of the pressure coefficient on upper and lower surface of the wing
C_L	local lift coefficient

σ, τ	parameters, independent of x
n	a number between 0 and 1
K_1, K_2	numbers, dependent on n (equation (9))
x'	variable of integration
a	a finite positive number, small compared with 1.

2. CALCULATION OF THE DOWNWASH

A standard co-ordinate system has been used: x in the direction of flight, y to starboard, and z vertically downwards (Fig. 1). An isolated infinite vortex line in the plane $z=0$ with a kink at $x=y=0$, swept back at an angle ϕ, induces a downwash velocity v_z in the plane $y=0$, given by

$$\frac{v_z(x, 0, z)}{V_0} = -\frac{\Gamma}{2\pi V_0 \cos\phi} \frac{x}{x^2+(z/\cos\phi)^2}\left[1-\sin\phi\frac{x}{\sqrt{(x^2+z^2)}}\right] \quad . \quad (1)$$

Γ is the strength of the vortex line; V_0 the velocity of the main flow. The downwash of a continuous distribution of such vortex lines of vorticity $\gamma(x)$ between $x=-1$ and $x=+1$ is obtained conveniently by integration in three parts as follows:

$$-2\pi V_0 \frac{v_z(x, 0, z)}{V_0} = I_1(x, 0, z)+I_2(x, 0,z)+I_3(x, 0, z) \quad . \quad . \quad (2)$$

$$\left.\begin{aligned} \text{where } I_1(x, 0, z) &= \int_{-1}^{+1}\gamma(x')\frac{x-x'}{(x-x')^2+(z/\cos\phi)^2}dx', \\ I_2(x, 0, z) &= -\sin\phi\int_{-1}^{+1}\frac{\gamma(x')}{[(x-x')^2+z^2]^{\frac{1}{2}}}dx', \\ I_3(x, 0, z) &= \sin\phi\int_{-1}^{+1}\frac{\gamma(x')(z/\cos\phi)^2}{\{(x-x')^2+(z/\cos\phi)^2\}[(x-x')^2+z^2]^{\frac{1}{2}}}dx'. \end{aligned}\right\} \quad . \quad (3)$$

The evaluation of these integrals requires some special care since the denominators of the integrands vanish at the point $x'=x$, $z=0$.

Putting $z=0$ before integrating is permissible for the first integral

$$I_1(x, 0, 0) = \int_{-1}^{+1}\gamma(x')\frac{dx'}{x-x'} \quad . \quad . \quad . \quad . \quad . \quad . \quad (4)$$

and the principal value has to be taken. This part corresponds to the well known expression for the downwash of a two-dimensional vortex distribution.

In treating the third integral, the range of integration is split into three parts; from -1 to $x-a$; from $x-a$ to $x+a$; and from $x+a$ to $+1$; a being a finite

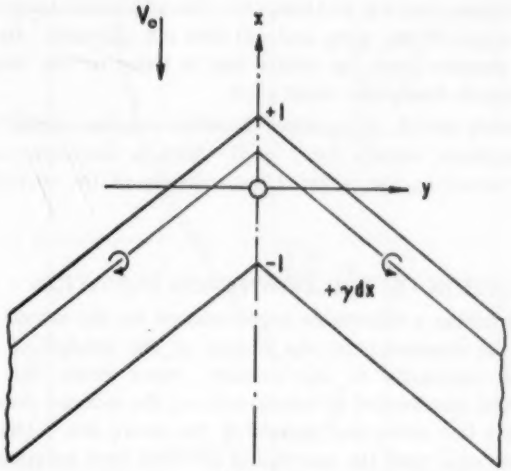

Fig. 1.

positive number, small compared with 1. In the first and last of these intervals the integrand has no singularity; therefore the limit as z tends to zero can be taken before integrating. Consequently these parts do not contribute to the downwash. Within the remaining interval $-a \leqslant x-x' \leqslant +a$ it is assumed that $\gamma(x')$ is a continuous function which can be replaced by its value at one point within the interval, at $x'=x$ say. I_3 can then be written as

$$I_3(x,\,0,\,0)=\sin\phi\,\gamma(x)\lim_{z\to 0}\int_{-a}^{+a}\frac{(z/\cos\phi)^2}{\{(x-x')^2+(z/\cos\phi)^2\}\,[(x-x')^2+z^2]^{\frac{1}{2}}}\,d(x-x'),$$

which gives

$$I_3(x,\,0,\,0)=\gamma(x)\lim_{z\to 0}\log_e\frac{[1+(z/a)^2]^{\frac{1}{2}}-\sin\phi}{[1+(z/a)^2]^{\frac{1}{2}}+\sin\phi},$$

so that finally

$$I_3(x,\,0,\,0)=\pi\,f(\phi)\,.\,\gamma(x) \qquad . \quad . \quad . \quad . \quad (5)$$

where

$$f(\phi)=\frac{1}{\pi}\log_e\frac{1-\sin\phi}{1+\sin\phi}.$$

This result does not depend on the actual value of a. The double limit $z\to 0$, $a\to 0$ gives the same result. Obviously z must tend to zero more rapidly than a, so that $z/a\to 0$. Otherwise the contributions of the first and third interval could not be ignored.

This additional downwash term depends on the local value of $\gamma(x)$ only, and corresponds exactly to the velocity increment v_z at the centre line of a thick swept

wing at zero incidence (*see e.g.* F. Ursell[1]). The additional downwash will spread over the centre region of the wing, and will fade out sideways. Its local value will depend on the distance from the centre line in terms of the wing chord. This additional downwash disappears when $\phi = 0$.

It is the second term I_2 in equation (3) which requires special treatment, since I_2 shows a logarithmic infinity for $z \longrightarrow 0$. Such a singularity cannot occur in practice. It is caused by the assumed discontinuity of the vorticity vector at the centre.

3. SIMPLIFICATION OF THE DOWNWASH EQUATION

One way of getting a reasonable approximation for the second downwash term is to calculate the downwash on the surface of the aerofoil of finite thickness. This leaves the singularity of the vorticity vector inside the profile section. Assuming a special distribution of bound vortices, the induced downwash has been calculated along a line above and parallel to the centre line. The result in Fig. 2 shows that, in this case, both the second and the third term are roughly proportional to the vortex distribution chosen. This result appears reasonable since the infinity of I_2 at $z = 0$ indicates that the vorticity in the immediate neighbourhood of the pivot point is of paramount influence.

A similar result will probably be obtained by rounding off the vortices at the centre, thus removing the discontinuity of the vorticity vector. Only a closed additional vortex of a strength proportional to $\gamma(x)$ of limited extent is needed to modify the kinked vortex line into a rounded one. Again, a finite value of the downwash will be obtained where one part should be proportional to the local vortex strength. An application of the method developed by Ursell[1] to this case might provide a proper solution to this problem.

In this note an approximate solution is attempted. Although the above estimates are not conclusive, they suggest that a downwash equation of the following form may be considered tentatively.

$$\frac{v_z(x)}{V_0} = -\frac{1}{2\pi V_0}\left\{\int_{-1}^{+1}\gamma(x')\frac{dx'}{x-x'} + \sigma\gamma(x)\right\} \text{ at } y=0, \quad . \quad . \quad (6)$$

where σ is a factor, dependent not on x but on the angle of sweep ϕ, and probably on the thickness ratio and shape of the aerofoil section. It is possible that, for very thin sections and kinked vortex lines, the value of σ tends to infinity. This would link equation (6) to the general equation (2). $\sigma = 0$ represents the case of the (two-dimensional) infinite sheared wing.

It is shown in Section 5 that the solutions of equation (6) agree with experiments, thus corroborating the suggested type of downwash equation.

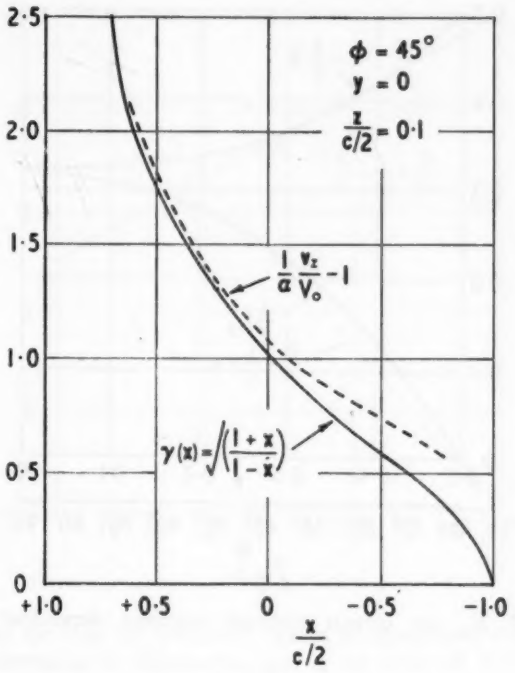

Fig. 2.

4. SOLUTION OF THE DOWNWASH EQUATION

The integral equation (6) has solutions of the following type,

$$\gamma(x)=2\alpha V_0 \cos\phi\, \tau \left(\frac{1+x}{1-x}\right)^n . \quad . \quad . \quad . \quad . \quad (7)$$

with $\gamma \longrightarrow \infty$ for $x=+1$ (leading edge), and $\gamma=0$ for $x=-1$ (trailing edge). τ is a factor, independent of x, and $0<n<1$. That $\gamma(x)$ is a solution of equation (6) can be seen from the fact that

$$\int_{-1}^{+1} \left(\frac{1+x'}{1-x'}\right) \frac{dx'}{x-x'} = K_1 + K_2 \left(\frac{1+x}{1-x}\right)^n . \quad . \quad . \quad . \quad (8)$$

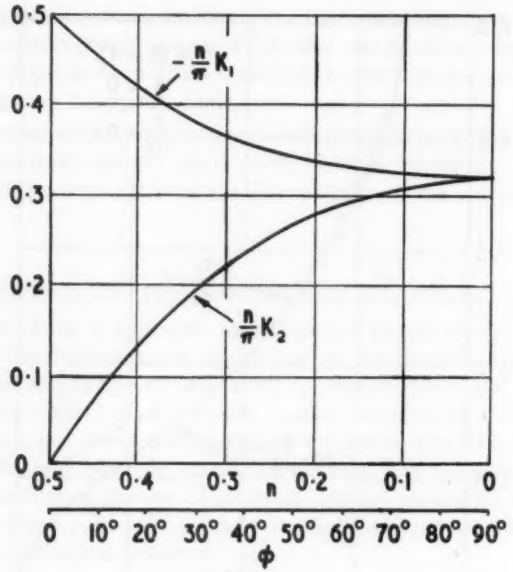

Fig. 3.

where K_1 and K_2 are certain constant numbers dependent only on the value of n, and

$$\left.\begin{aligned} K_1 &= -\frac{1}{n}\int_0^\infty \frac{1}{1+s^{1/n}}\,ds, \\ K_2 &= \frac{1}{n}\int_0^\infty \frac{1}{1-t^{1/n}}\,dt. \end{aligned}\right\} \quad . \quad . \quad . \quad . \quad . \quad . \quad (9)$$

The transformations

$$s=\left(\frac{1+x'}{1-x'}\right)^n, \qquad t=s\left(\frac{1+x}{1-x}\right)^{-n}$$

have been used. Numerical values of K_1 and K_2 are plotted in Fig. 3. In particular

$K_1=-\pi$; $K_2=0$ for $n=\frac{1}{2}$ (two-dimensional flat plate),
$K_1=-\pi\sqrt{2}$; $K_2=\pi$ for $n=\frac{1}{4}$,
$nK_1=-1$; $nK_2=1$ for $n=0$.

5. APPROXIMATE VALUES FOR THE EXPONENT n

It is doubtful whether reasonable values for the parameter τ can be obtained from equations (6) and (7) since the effect of the trailing vortices has been

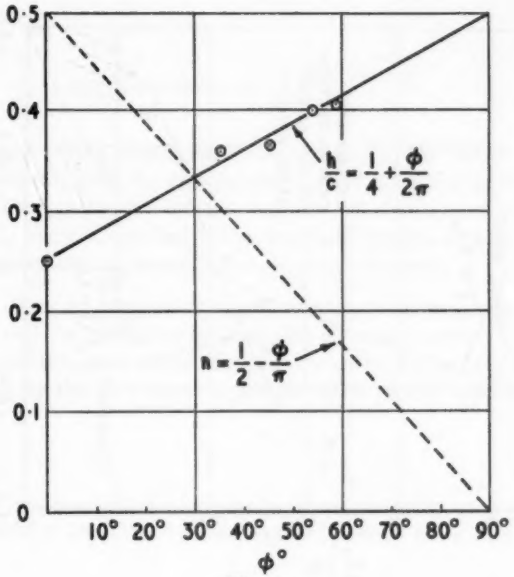

Fig. 4.

ignored, so that the total lift coefficient cannot be determined this way. But the shape of the chordwise lift distribution, that is the value of n, can be estimated more easily by using some experimental data. This estimate makes use of the simple fact that the aerodynamic centre of the vortex distribution (7) is given by

$$h/c=(1-n)/2, \quad n=1-2h/c, \qquad . \quad . \quad . \quad . \quad (10)$$

where h is the distance of the aerodynamic centre from the leading edge. Experimental results in Fig. 4 suggest that

$$h/c=\tfrac{1}{4}+\phi/(2\pi). \qquad . \quad . \quad . \quad . \quad . \quad . \quad (11)$$

is a sufficiently accurate approximation for the relation between the aerodynamic centre position at the centre-section and the angle of sweep.

Combining equations (10) and (11)

$$n=\tfrac{1}{2}-\phi/\pi. \qquad . \quad . \quad . \quad . \quad . \quad . \quad . \quad (12)$$

Thus $n=\frac{1}{2}$ for the unswept (or infinite sheared) wing (flat plate),

$0<n<\frac{1}{2}$ for the centre of swept-back wings,

$\frac{1}{2}<n<1$ for the centre of swept-forward wings.

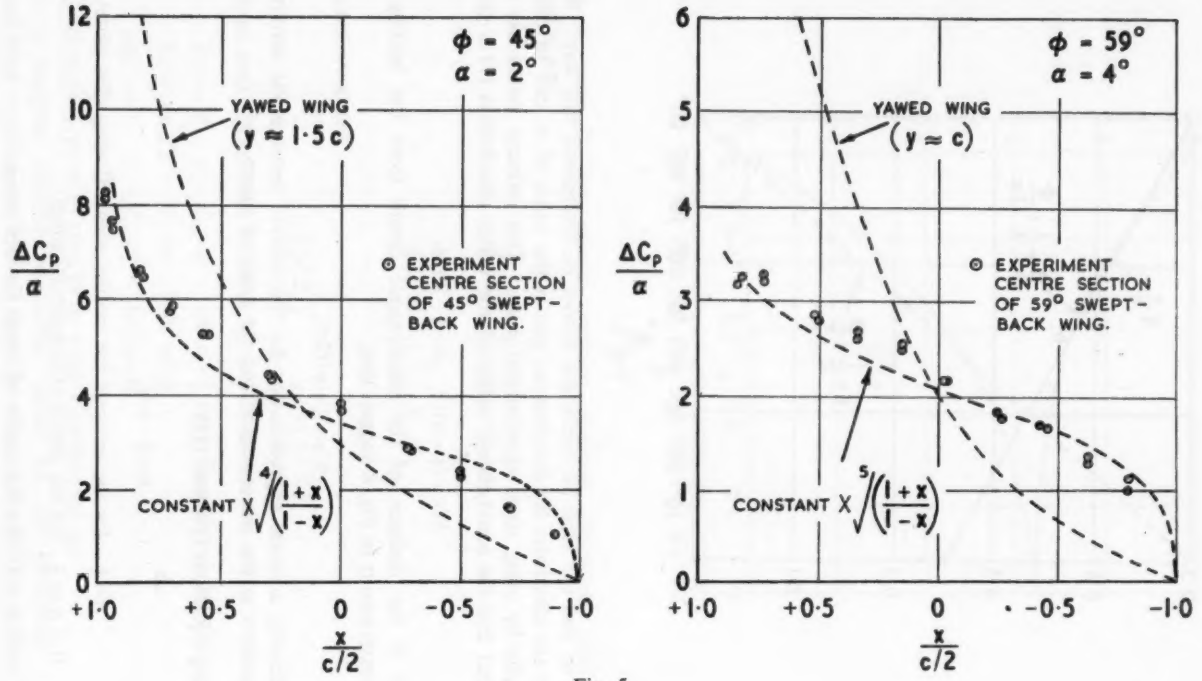
φ = 45°
α = 2°
YAWED WING
(y ≈ 1·5 c)
⊙ EXPERIMENT
CENTRE SECTION
OF 45° SWEPT-
BACK WING.
CONSTANT X $\sqrt[4]{\left(\frac{1+x}{1-x}\right)}$
$\frac{\Delta C_p}{\alpha}$
$\frac{x}{c/2}$
+1·0
+0·5
0
-0·5
-1·0
φ = 59°
α = 4°
YAWED WING
(y ≈ c)
⊙ EXPERIMENT
CENTRE SECTION
OF 59° SWEPT-
BACK WING.
CONSTANT X $\sqrt[5]{\left(\frac{1+x}{1-x}\right)}$

Fig. 5.

ERRATA

The function

$$\gamma(x) = \text{constant} \times \left(\frac{1+x}{1-x}\right)^{\frac{1}{2}\left(1-\frac{\phi}{\pi/2}\right)} \quad . \quad . \quad . \quad . \quad (13)$$

represents the type of the chordwise lift distribution at the centre of swept wings fairly well, considering that the approximation is of the same order as that of the flat-plate distribution in the two-dimensional case. A comparison with experimental results in Fig. 5, where a constant factor has been applied to give the right value of C_L, shows reasonable agreement.

It is to be expected that, in moving outwards from the centre, the chordwise lift distribution will change gradually from that given by equation (13) at the centre to a flat-plate distribution, at about one chord from the centre, *i.e.* from $n = \frac{1}{2} - \phi/\pi$ to $n = \frac{1}{4}$. The wing tips will show a similar effect in the opposite direction, *i.e.* $n > \frac{1}{4}$.

REFERENCES

1. URSELL, F. (1948). Notes on the Linear Theory of Incompressible Flow round Symmetrical Swept-Back Wings at Zero Lift. *The Aeronautical Quarterly*, Vol. I, May 1949, pp. 101-122.

ERRATA

Amendments to "A Note on the Bending Moment Induced in the Booms of a Spar at the Point of Application of a Concentrated Load." (Part IV, Volume I, February 1950).

10*th May* 1950

I regret that in my note on the above subject, published in *The Aeronautical Quarterly*, February 1950, some errors have come to light.

I would be most grateful if the corrections could be given publicity, and I am accordingly enclosing a statement of the corrections.

H. F. WINNY,
Head of Technical Department,
The Fairey Aviation Co. Ltd.

Page 285. Line 5. Replace $3\alpha^2 - \beta^2$ by $\dfrac{3\alpha^2 - \beta^2}{\alpha}$

and $\alpha^2 - 3\beta^2$ by $\dfrac{\alpha^2 - 3\beta^2}{\beta}$

Line 18. Replace $\left(\frac{\alpha^2+\beta^2}{\alpha\beta}\right)$ by $\frac{(\alpha^2+\beta^2)^2}{\alpha\beta}$

Line 19. Replace $(\alpha^2+\beta^2)$ by $(\alpha^2+\beta^2)^2$

Line 22. Replace $\frac{\alpha^2+\beta^2}{\beta}$ by $\frac{\alpha^2+\beta^2}{\alpha}$

and K in numerator by $K^{\frac{1}{2}}$.

Page 286. Replace existing Fig. 2 by new Fig. 2.

Page 287. Line 1. Replace α/β by β/α.

Line 3. Replace $\sqrt{\frac{K+1}{K-1}}$ by $\frac{1}{2}\sqrt{\frac{K+1}{K-1}}$

Page 288. Line 3. Replace K in numerator by $K^{3/2}$.

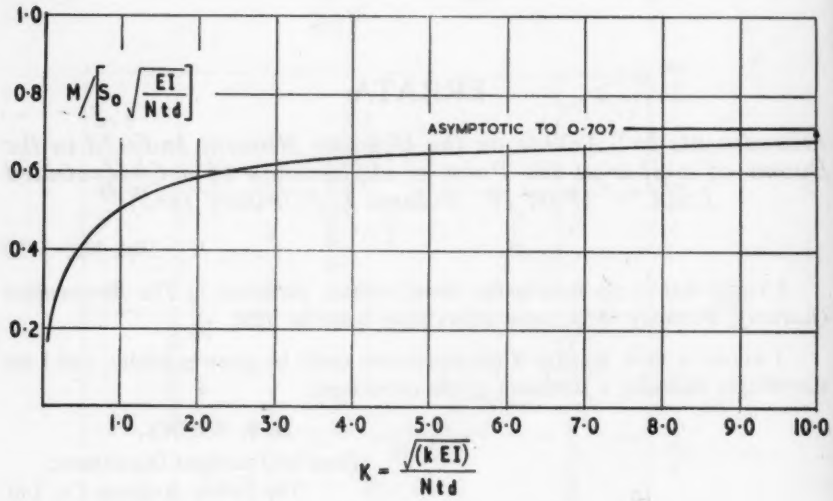

Fig. 2.
Maximum bending moment carried by boom.